

Mechanistic Interrogation of Alkyne Hydroarylations Catalyzed by Highly Reduced, Single-Component Cobalt Complexes

Benjamin A. Suslick, and T. Don Tilley

J. Am. Chem. Soc., **Just Accepted Manuscript** • DOI: 10.1021/jacs.0c04072 • Publication Date (Web): 26 May 2020

Downloaded from pubs.acs.org on May 27, 2020

Just Accepted

“Just Accepted” manuscripts have been peer-reviewed and accepted for publication. They are posted online prior to technical editing, formatting for publication and author proofing. The American Chemical Society provides “Just Accepted” as a service to the research community to expedite the dissemination of scientific material as soon as possible after acceptance. “Just Accepted” manuscripts appear in full in PDF format accompanied by an HTML abstract. “Just Accepted” manuscripts have been fully peer reviewed, but should not be considered the official version of record. They are citable by the Digital Object Identifier (DOI®). “Just Accepted” is an optional service offered to authors. Therefore, the “Just Accepted” Web site may not include all articles that will be published in the journal. After a manuscript is technically edited and formatted, it will be removed from the “Just Accepted” Web site and published as an ASAP article. Note that technical editing may introduce minor changes to the manuscript text and/or graphics which could affect content, and all legal disclaimers and ethical guidelines that apply to the journal pertain. ACS cannot be held responsible for errors or consequences arising from the use of information contained in these “Just Accepted” manuscripts.

Mechanistic Interrogation of Alkyne Hydroarylations Catalyzed by Highly Reduced, Single-Component Cobalt Complexes

Benjamin A. Suslick and T. Don Tilley*

Department of Chemistry, University of California, Berkeley, California 94720, United States

Chemical Sciences Division, Lawrence Berkeley National Laboratory, Berkeley, California 94720, United States

Supporting Information Placeholder

ABSTRACT: Highly reactive catalysts for *ortho*-hydroarylations of alkynes have previously been reported to result from activation of CoBr₂ by Grignard reagents, but the operative mechanism and identity of the active cobalt species have been undefined. A mechanistic analysis of a related system, involving hydroarylations of a (*N*-aryl)aryl ethanimine with diphenylacetylene, was performed using isolable reduced Co complexes. Studies of the stoichiometric reaction of Co(I) or Co(II) precursors with CyMgCl implicated catalyst initiation via a β-H elimination/deprotonation pathway. The resulting single-component Co(-I) complex is proposed as the direct precatalyst. Michaelis-Menten enzyme kinetic studies provide mechanistic details regarding the catalytic dependence on substrate. The (*N*-aryl)aryl ethanimine substrate exhibited saturation-like behavior whereas alkyne demonstrated a complex dependency; rate inhibition and promotion depends on the relative alkyne to imine concentration. Activation of the aryl C–H bond occurred only in the presence of coordinated alkyne, which suggests operation of a concerted metalation-deprotonation (CMD) mechanism. Small primary isotope effects are consistent with a rate-determining C–H cleavage. Off-cycle olefin isomerization catalyzed by the same Co(-I) active species appears to be responsible for the observed *Z*-selectivity.

INTRODUCTION

Chelation-assisted C–H activations allow selective functionalization of unreactive C–H bonds, thereby accessing atom-economical, late-stage molecular modifications without the installation of wasteful cross-coupling partners.^{1–9} In this context, hydroarylation has emerged as an attractive method to form C–C bonds *via* the addition of activated aryl C–H bonds across olefins or alkynes. In the past two decades, catalyst development for such reactions has been aided by mechanistic investigations.^{2,8–10} The first report of olefin hydroarylation from the Murai group^{11,12} described RuH₂(CO)(PPh₃)₃ as the precatalyst and more recent advances in hydroarylations are based on precatalysts bearing a metal center with a square-planar, d⁸ or octahedral d⁶ configuration (e.g., Rh(I),^{13–18} Ir(I)^{19–28} Pd(II),²⁹ and Pt(II)^{30–32}). Significantly, mechanistic studies with these second- and third-row transition metal catalysts implicate a rate-limiting C–H addition.^{30–33} By comparison, far fewer first-row transition metal hydroarylation catalysts have been identified, despite recent efforts to exploit the high abundance and low costs³⁴ of Fe,³⁵ Co,^{3,36} and Ni.^{37–42} Future catalyst designs should rely on mechanistic information that is largely nonexistent, and notably, first-row metals often engage in mechanisms that are distinctly different from those of heavier transition metals.^{2,5,43}

Recent developments in Co-catalyzed *ortho*-hydroarylations illustrate the potential for highly active first-row transition

metal complexes to participate in C–H activation chemistry.^{36,44–54} Two distinct classes of Co precatalysts have been discovered, based on either high- or low-valent cobalt. For well-defined, high-valent Co(III) complexes, DFT calculations suggest that a redox-neutral C–H activation step is plausible.^{44–46,55,56} Additionally, the isolation of cyclometallated intermediates implicate the operation of an alkyne insertion step in the catalytic cycle.^{45,55} In comparison, mechanisms for low-valent Co catalysis remain elusive.

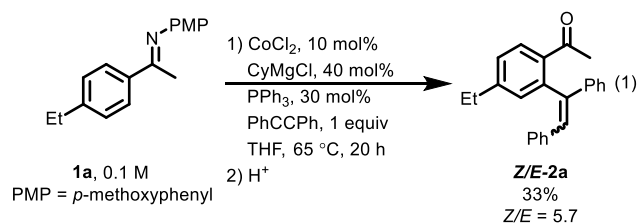
Low-valent cobalt catalysts for the hydroarylation of alkynes have been generated *in situ* and have been extensively studied by the Yoshikai group.^{36,47–53} The uncharacterized, active catalytic species is generated by treatment of CoBr₂ with certain Grignard reagents (e.g., ^tBuCH₂MgBr and Me₃SiCH₂MgBr) in the presence of added ligands and substrates. Additionally, the resultant hydroarylation products form as a mixture of *E*- and *Z*-olefins and this aspect of the mechanism is also not understood.

Several plausible catalytic cycles have been proposed for the catalytic hydroarylation of (*N*-aryl)aryl ethanimines with internal alkynes;³⁶ however, specific details about the nature of the catalytic intermediates (e.g., oxidation states, ligand sphere, etc.) or the initiation pathway have remained unclear. The Grignard reagent has been proposed to reduce the Co(II) precatalyst to a Co(I) or Co(0) active species, possibly *via* a radical-based, one-electron reductive coupling.^{2,3} While metal-hydride

complexes are implicated as key intermediates, such species have yet to be observed. The work described here addresses the mechanism of alkyne hydroarylation by low-valent cobalt, with reactivity studies that provide insight into the nature of the catalytically active species, the catalytic cycle, and the concurrent olefin isomerization.

RESULTS AND DISCUSSION

Conditions for Catalytic Hydroarylation. Investigations began with examination of a particular “one-pot” transformation closely related to those described by Yoshikai and coworkers³⁶ involving hydroarylation of diphenylacetylene by an (*N*-aryl)aryl ethanimine, with a CoCl₂/RMgCl (R = -CH₂CMe₃, -CH₂SiMe₃)/P(3-Cl-C₆H₄)/pyridine catalyst system. For these reactions, reported yields range from 60-95% and strongly favor the *E*-isomer as the product (*Z/E* ratio of ca. 0.1-0.2). The reaction chosen for study also utilized an *in situ*-generated catalyst from a CoCl₂/CyMgCl/PPh₃ mixture. In this case, the hydroarylation of **1a** was found to proceed in 33% yield, but surprisingly with *Z*-selectivity and a relatively high *Z/E* ratio of 5.7 after hydrolysis (eq 1). It is worth noting that *Z*-selective catalysis has also been observed by the Petit group⁵⁷ using Co(I)-PMe₃ precatalysts and microwave conditions.



Previous reports of such reactions speculated that the reducing conditions likely give rise to a low-valent catalytically active species formed by the reduction of Co(II) precursors by the Grignard reagent.^{2,3,36,47} To more thoroughly probe the nature of the active catalyst, the well-defined Co(I) complex (PPh₃)₃CoCl⁵⁸ (**Co-Cl**) was investigated as a catalyst precursor. Complex **Co-Cl** is not a competent single-component hydroarylation catalyst (Table 1); however, treatment of **Co-Cl** with two equivalents of CyMgCl produced a catalytic species giving yields similar to those observed with CoCl₂/PPh₃ in the presence of activators (eq 1). Since previous reports have indicated a dramatic effect associated with the nature of the Grignard reagent,^{36,47} catalysis with **Co-Cl** was examined with a range of organometallic activators (Table 1). The best results were obtained with CyMgCl, and in general it appears that β-hydrogens in the alkyl group of the magnesium reagent lead to better results.

In general, organomagnesium reagents were observed to out-perform more reactive organolithium reagents. In some cases, no catalysis resulted from treatment of **Co-Cl** with an organolithium. In contrast to results reported by the Yoshikai group^{36,47-53} where *E*-products are favored (*vide supra*), the *Z*-isomer (formally a *trans*-insertion product) is the major species with all the activators tested. Additionally, the degree of *Z*-selectivity was found to vary with the organometallic activator employed. Activators bearing β-CH₂ fragments (e.g., EtMgCl,

CyMgCl, or ⁿBu₂Mg) successfully activated **Co-Cl** towards productive catalysis.

Table 1. Effects of Organometallic Activator Identity.

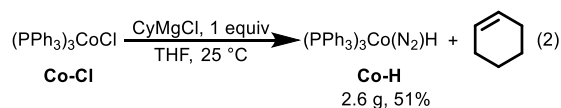
M-R	¹ H NMR Yield (%) ^a	Z/E ^a
–	0	–
ⁿ BuLi	5	4.4
PhLi	< 2	–
MesLi	12	33
MeMgCl	< 2	–
EtMgCl	32	5.1
H ₂ C=CHMgBr ^b	33	27
CyMgCl	33	> 100
CyMgCl ^b	84	> 100
ⁿ Bu ₂ Mg	55	> 100
Mes ₂ Mg	10	14
Bn ₂ Mg	41	5.2
Ph ₂ Zn	5	23

^a As measured by ¹H NMR spectroscopy of the crude reaction mixture vs Si(SiMe₃)₄ as an internal standard. ^b An equivalent of pyridine was added.

Optimization of catalytic conditions with **Co-Cl** and CyMgCl revealed several insights. First, Yoshikai and coworkers³⁶ observed that addition of an equivalent of pyridine greatly improved yields (a two-fold increase in some cases). Similarly, addition of 1 equiv of pyridine (relative to substrates) to a catalytic mixture derived from **Co-Cl**/CyMgCl improved ¹H NMR yields from 33 to 84% (Supporting Information, Table S4). Also, catalytic efficiencies modestly improved with addition of 5% v/v TMEDA or 1,4-dioxane, to 45 and 42%, respectively (Table S4). The possible role of adventitious acid in this catalysis (e.g., to facilitate a Friedel-Crafts processes) was addressed by addition of one equivalent (relative to Co) of a proton scavenger. Thus, the non-coordinating base 2,6-di-*tert*-butyl-4-methylpyridine was added in lieu of pyridine to the catalytic mixture. This experiment illustrates that the catalytic yield is unaffected by the presence of this compound (Table S4). The addition of these weakly Lewis basic additives (*i.e.*, Py, TMEDA, 1,4-dioxane) likely aids in the separation of the Li⁺ or Mg²⁺ counterions from the anionic metal center *via* the formation of a crowned complex, thereby increasing the nucleophilicity at Co. However, stoichiometric addition (relative to Co) of strongly coordinating *N*-heterocyclic carbene ligands (e.g., IMes or IPr) in the presence or absence of pyridine resulted in complete catalytic inhibition (Table S4). Inhibition of catalysis also occurred in coordinating solvents (e.g., Py or MeCN). On the other hand, ethereal solvents (THF, 2-methyl-THF, dioxane, Et₂O) resulted

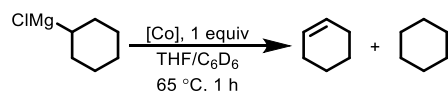
in the highest catalytic conversions (Supporting Information, Table S5). The CyMgCl/Co-Cl ratio (in THF with pyridine) was found to impact both conversion and selectivity in catalysis (Supporting Information, Table S6). While at least two equivalents of CyMgCl relative to Co were required for reasonable conversion, an excess of ca. 5 equiv of CyMgCl greatly reduced activity by adventitious substrate degradation *via* nucleophilic attack. Finally, the concentration of the substrate influenced the overall conversion (Supporting Information, Table S7); dilute catalytic conditions provided the highest yielding *in situ* catalyst, and yields decreased as a function of substrate concentration (e.g., 83% for 0.05 M vs. 66% for 1.0 M, as measured by ^1H NMR spectroscopy).

Formation and Identity of Catalytically Active Species. The activation of cobalt by the organomagnesium reagent would seem to occur *via* formation of a reactive alkyl complex of the type $(\text{PPh}_3)_3\text{CoR}$. Interestingly, treatment of **Co-Cl** with 1 equiv of CyMgCl (eq 2) cleanly produced cyclohexene and the diamagnetic hydride $(\text{PPh}_3)_3\text{Co}(\text{N}_2)\text{H}$ (**Co-H**), first reported by Sacco and Rossi^{59,60} in 1967.



It has been previously reported by Kisch and coworkers⁶¹ that **Co-H** catalyzes the hydroarylation of diphenylacetylene with diaryl-substituted diazo compounds as a neat melt at 85 $^\circ\text{C}$. However, in our hands, 10 mol% of complex **Co-H** did not promote catalysis with diphenylacetylene and **1a** in a solution of THF and pyridine heated to 65 $^\circ\text{C}$ for 1 d. However, the addition of an equiv (relative to Co) of CyMgCl or a similarly strong base (e.g., $^n\text{BuLi}$, LDA) gave catalysis (Supporting Information, Table S8). Activation of the cobalt hydride species under the latter conditions suggests that the active catalyst results from deprotonation.

Table 2. Quantification of Cyclohexene and Cyclohexane from Activation of Cobalt Species.

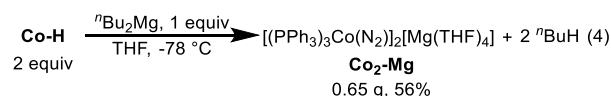
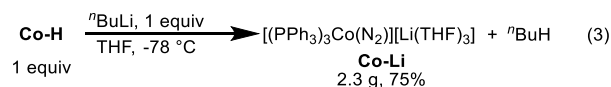


[Co]	CyMgCl (equiv)	Cyclohexene (equiv) ^a	Cyclohexane (equiv) ^a
$\text{CoCl}_2/3\text{PPh}_3$	1	0.7	0.3
	2	1	1
	4	2	2
Co-Cl	1	0.7	0.3
	2	1	1
	4	1	1
Co-H	1	0	1

^a Volatile organic products were separated from [Co] via vacuum transfer and quantified by ^1H NMR spectroscopy vs *p*-xylene as an internal standard.

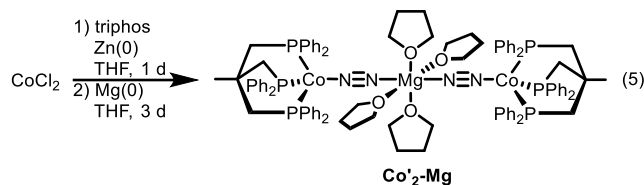
The organic byproducts created by treatment of complexes **Co-Cl** and **Co-H** (as well as $\text{CoCl}_2/3\text{PPh}_3$) with CyMgCl were quantified by ^1H NMR spectroscopy (Table 2). With two equivalents of CyMgCl , equimolar amounts of cyclohexene and cyclohexane were observed for both CoCl_2 (with PPh_3) and **Co-Cl**. An excess of CyMgCl with **Co-Cl** did not result in the evolution of additional cyclohexene or cyclohexane. In contrast, stoichiometric treatment of **Co-H** with CyMgCl afforded only a single equivalent of cyclohexane.

Upon first inspection, it is perhaps surprising that deprotonation of **Co-H** occurs given the ancillary ligand environment, since cobalt hydride complexes bearing only σ -donating phosphine co-ligands display hydridic character (e.g., $\text{p}K_a^{\text{MeCN}}[\text{HCo}(\text{dppe})_2] = 38.1$). The introduction of π -acidic ligands considerably reduces the $\text{p}K_a$ value (e.g., $\text{p}K_a^{\text{MeCN}}[\text{HCo}(\text{CO})_4] = 8.3$; $[\text{HCo}(\text{CO})_3(\text{PPh}_3)] = 15.4$).^{62,63} Given the slight π -acidic behavior of end-on N_2 ligands, it seems plausible that **Co-H** is deprotonated with a strong base such as a RMgX or R_2Mg (e.g., $\text{p}K_a^{\text{THF}}[\text{EtMgCl}] = 30.1$; $\text{p}K_a^{\text{THF}}[\text{Et}_2\text{Mg}] = 30.5$).⁶⁴ Indeed, stoichiometric treatment of **Co-H** with MeLi , $^n\text{BuLi}$, Bn_2Mg , or CyMgCl generated an equivalent of the corresponding alkane (i.e., MeH , ^nBuH , toluene, and CyH , respectively) as determined by ^1H NMR spectroscopy in benzene- d_6 . Gram-scale deprotonation of **Co-H** with $^n\text{BuLi}$ or $^n\text{Bu}_2\text{Mg}$ in THF (eqs 3 and 4) afforded $\text{Co}(\text{I})$ complexes of the type $[(\text{PPh}_3)_3\text{Co}(\text{N}_2)]_n\text{M}$ ($\text{M} = \text{Li}(\text{THF})_3$, $n = 1$, **Co-Li**; $\text{M} = \text{Mg}(\text{THF})_4$, $n = 2$, **Co}_2\text{-Mg}**) as reported by Yamamoto and coworkers.⁶⁵



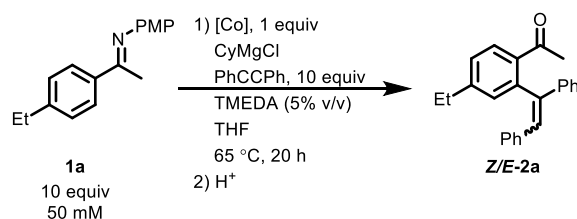
Complexes **Co-Li** and **Co}_2\text{-Mg}** exhibit red-shifted N_2 stretching modes at 1898 and 1860 cm^{-1} , respectively (for comparison, $\nu_{\text{N-N}}(\text{Co-H}) = 2092 \text{ cm}^{-1}$; KBr). **Co-Li** exhibited a broad $^7\text{Li}\{^1\text{H}\}$ NMR resonance at -3.8 ppm in benzene- d_6 , which is consistent with solvent-separated ion pairs.⁶⁶⁻⁶⁸ Hydrolysis of **Co-Li** resulted in liberation of three equivalents of both THF and PPh_3 as determined by ^1H NMR spectroscopy versus $\text{Si}(\text{SiMe}_3)_4$ as an internal standard, which is in agreement with the solid-state composition of **Co-Li** as determined by elemental analysis. However, both complexes appear to exhibit ligand dissociation in benzene- d_6 , as indicated by the existence of a $^{31}\text{P}\{^1\text{H}\}$ NMR resonance at -5.24 ppm (unbound PPh_3), along with those for **Co-Li** (48.14) or **Co}_2\text{-Mg}** (48.26).

For comparative purposes, a structural analogue to **Co}_2\text{-Mg}** was prepared according to the procedure described by Long and coworkers.⁶⁹ Treatment of CoCl_2 with Zn and the tridentate ligand triphos, $\text{MeC}(\text{CH}_2\text{PPh}_2)_3$, afforded the intermediate species $[(\text{triphos})\text{CoCl}]$, which upon further reduction with Mg afforded **Co}'_2\text{-Mg}** (eq 5). This complex exhibits a similarly red-shifted N_2 stretch at 1846 cm^{-1} (KBr). Complex **Co}'_2\text{-Mg}** gives rise to a single $^{31}\text{P}\{^1\text{H}\}$ NMR resonance at 31.20 ppm.



6 While complexes of Co(-I) are relatively uncommon, a recent report by Deng and coworkers⁷⁰ describes the Co(-I) dinitrogen complex [(ICy)₂Co(N₂)₂][K(18-c-6)] in the context of nitrogen fixation. DFT calculations indicate that the formally d¹⁰ Co center engages in extensive back-bonding into the N₂ π* orbital, which may activate the N₂ ligand of this complex for functionalization. An example of such reactivity is borne out in the catalytic silylation of N₂ to N(SiMe₃)₃ in the presence of excess KCo and Me₃SiCl.⁷⁰ Long and coworkers⁵⁹ described similar N₂ functionalization chemistry with Co'-2-Mg; stoichiometric treatment of this complex with Me₃SiCl afforded the silyldiazenido complex, [(triphos)Co(N₂SiMe₃)], likely as a result of N₂ activation by the electron rich metal center. Given this notable reactivity toward N₂, investigations into interactions of highly-reduced Co complexes with unsaturated substrates (i.e., olefins and alkynes) are of interest, particularly in the context of hydroarylations.

7
8
9
10
11
12
13
14
15
16
17
18
19
20
21
22
23 **Table 3. Activity Comparison of Added Catalysts.**



[Co]	CyMgCl (equiv)	¹ H NMR Yield (%) ^a	Z/E ^a
CoCl ₂ /3PPh ₃	4	41	40
Co-Cl	0	0	–
	2	45	59
Co-H	0	0	–
	1	44	65
Co-Li	0	58 (50) ^b	> 100
Co ₂ -Mg ^{c,d}	0	64 (48) ^b	44
Co'-2-Mg ^{c,d}	0	0	–

32
33
34
35
36
37
38
39
40
41
42
43
44
45
46
47
48
49

^a Determined by comparison to a known quantity of Si(SiMe₃)₄ as an internal standard. ^b Isolated yield given in parenthesis. ^c 0.5 equiv of complex was added. ^d 1,4-dioxane (5% v/v) was used instead of TMEDA.

50
51
52
53
54
55
56
57
58
59
60

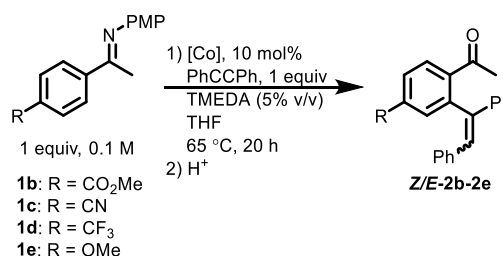
Table 3 compares the catalytic hydroarylation activity of cobalt complexes **Co-Cl**, **Co-H**, **Co-Li**, **Co₂-Mg**, and **Co'-2-Mg** with those of a catalyst generated *in situ* as described above in eq 1. TMEDA or 1,4-dioxane were employed as co-solvents in place of pyridine since higher catalytic activities for the anionic complexes were observed under those conditions, presumably

by enhanced Li or Mg sequestration. While neither **Co-Cl** nor **Co-H** are single-component catalysts, competent catalysis occurs after addition of CyMgCl (1 and 2 equiv, respectively). In contrast to the Co(I) precursors, the Co(-I) species **Co-Li** and **Co₂-Mg** catalytically coupled (*N*-aryl)aryl ethanimine **1a** and diphenylacetylene without the addition of Grignard. Additionally, catalytic yields observed for **Co-Li** and **Co₂-Mg** are comparable to those obtained using CoCl₂/3PPh₃, **Co-Cl**, or **Co-H** with a corresponding quantity of CyMgCl, which implicates [(PPh₃)₃Co(N₂)]⁻ as the catalytically active Co fragment. Interestingly, **Z-2a** was the major isomer observed regardless of precatalyst, which suggests that a common species capable of *E*- to *Z*-olefin isomerization exists as a result of activation with CyMgCl.

Unlike the PPh₃-ligated complexes, the triphos analogue **Co'-2-Mg** did not catalyze hydroarylation. Stoichiometric reactions with either diphenylacetylene or **1a** did not consume the organic substrate and instead afforded a common, unknown paramagnetic species consistent with broadened ¹H NMR resonances at δ 15.10 (br s, 18H), -1.17 (br s, 6H), -2.54 (br s, 2H) in benzene-*d*₆ (see Supporting Information, Figures S4 and S5). The lack of reactivity with alkyne or aryl-imine observed with **Co'-2-Mg** implies that a catalytic intermediate with fewer than three ancillary phosphine ligands is required for catalysis.

While hydroarylations reported by the Yoshikai group³⁶ have focused on Mg-containing activators, **Co-Li** proved to be more convenient for mechanistic investigations. The charge matching of the Co(-I) fragment and Li⁺ is expected to result in more facile ion dissociation events as compared to **Co₂-Mg**. All subsequent mechanistic studies, therefore, employed **Co-Li** as the catalyst.

32
33
34
35
36
37
38
39
40
41
42
43
44
45
46
47
48
49
50
51
52
53
54
55
56
57
58
59
60 **Table 4. Arene Functional Group Tolerance.**



Imine	[Co]	Yield (%) ^{a,b}	Conv. (%) ^{a,c}	Z/E ^a
1b	CoCl ₂ /3PPh ₃ /4CyMgCl	30	68	8.8
	Co-Li	36 (33)	36	8.0
1c	CoCl ₂ /3PPh ₃ /4CyMgCl	11	36	> 100
	Co-Li	86 (70)	86	6.7
1d	Co-Li	43 (29)	43	15
1e	Co-Li	47 (27)	47	20

^a ¹H NMR yield and Z/E ratios were determined by comparison to a known quantity of Si(SiMe₃)₄ as an internal standard. ^b Isolated yield given in parenthesis. ^c Conversion was determined from

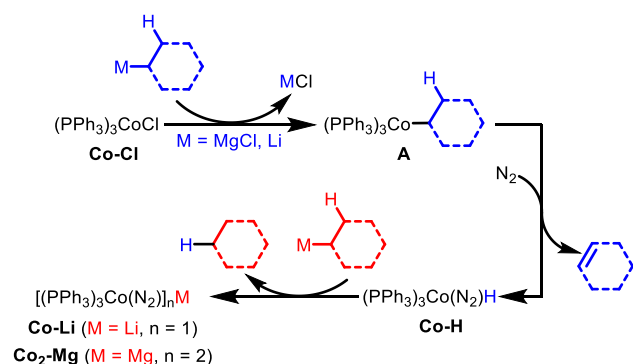
the quantity of substituted acetophenone derived from hydrolysis of unreacted imine substrate.

Comparisons of the functional group tolerance of the single-source catalyst **Co-Li** vs. the *in situ* $\text{CoCl}_2/3\text{PPh}_3/\text{CyMgCl}$ catalyst were made for several substrates as shown in Table 4. These results illustrate a potential advantage to “Grignard-free” hydroarylations. Electrophilic groups (e.g., esters, ketones, aldehydes) are often not compatible with nucleophilic organomagnesium reagents that can undergo rapid, competing reactions with the substrate. This problem may be circumvented to some extent by addition of the Grignard to the catalyst mixture prior to introduction of the substrate, but *in situ* catalyst generations of this type often employ a slight excess of activator. Note that the Yoshikai group⁵² has developed “Grignard-free” catalysis by use of Mg turnings as the terminal reductant, but these reducing conditions may also lead to undesired reactions of various functional groups (e.g., halides).

Significantly, with complex **Co-Li** as the catalyst, substrates bearing an ester (**1b**) or a nitrile (**1c**) group are tolerated in modest yields; only the desired product was observed. In contrast, the *in situ* reactions did not cleanly catalyze hydroarylation since products derived from nucleophilic addition of CyMgCl to the carbonyl or nitrile fragments were produced, as observed by ^1H NMR spectroscopy. The existence of such species requires more difficult purification procedures. Moderate catalytic conversion occurred with substrates bearing electron-withdrawing CF_3 (**1d**) or donating OMe (**1e**) functionalities. These data suggest that complex **Co-Li** may be useful for substrates that are not tolerated by the catalysts generated *in situ* despite being mildly acid-sensitive.

Given the observations described above, it appears that catalyst generation occurs by treatment of precatalyst **Co-Cl** with an organometallic transmetalation reagent bearing a $\beta\text{-H}$ substituent (e.g., EtMgCl , CyMgCl , etc; Scheme 1). The resultant Co-R complex (**A**) undergoes rapid $\beta\text{-H}$ elimination under an N_2 atmosphere to generate $(\text{PPh}_3)_3\text{Co}(\text{N}_2)\text{H}$ (**Co-H**) and an equivalent of olefin (e.g., ethylene, cyclohexene, etc.). Deprotonation by the basic organometallic activator then results in formation of stoichiometric alkane (e.g., ethane or cyclohexane) and the active $\text{Co}(\text{I})$ anion. Indeed, similar activation pathways have been reported by Koszinowski and coworkers⁷¹ in the context of Co -catalyzed Heck-type reactions.

Scheme 1. Proposed Catalyst Activation Mechanism.



Substrate Binding and Implications for the Catalytic Cycle.

To probe interactions of the alkyne substrate with the cobalt center, **Co-Li** was treated with an excess of the alkyne bis(*para*-tolyl)acetylene (*p*-TolCCp-Tol; Figure 1). For varying quantities of added alkyne, the ratio of free to bound alkyne was quantified vs. an internal standard after equilibration. The existence of multiple distinct tolyl-CH₃ resonances suggests the presence of a mixture of several alkyne-ligated complexes. On the basis of the initial concentration of **Co-Li**, an average number of bound alkynes per Co (x) was determined for various $[\text{p-TolCCp-Tol}]_0/[\text{Co-Li}]_0$ ratios and temperatures, and the results are plotted in Figure 1. The addition of alkyne results in displacement of ligated PPh_3 , and under catalytic conditions (ca. 10 equivs relative to Co) ~ 2 alkynes per Co are consumed, which corresponds to displacement of the N_2 ligand and one PPh_3 . Surprisingly, this ratio appears to be temperature invariant.

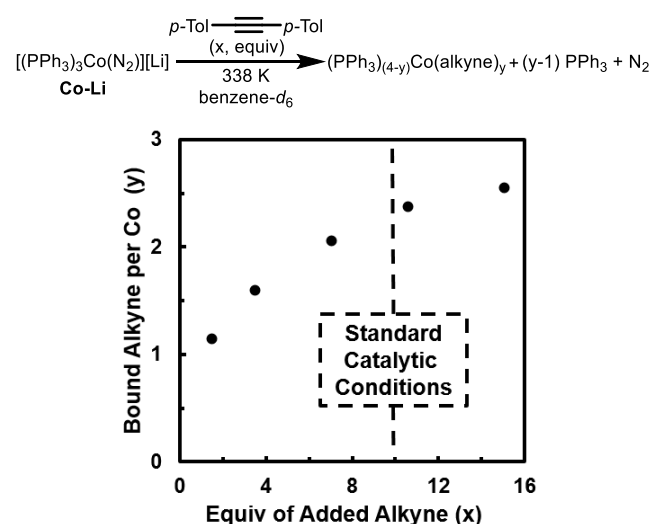


Figure 1. Average bound alkynes per Co as a function of alkyne equivalents. Reaction conditions: $[\text{Co-Li}]_0 = 13$ mM; $[\text{bis}(\text{p-tolyl})\text{acetylene}]_0 = 19, 44, 90, 135,$ and 190 mM. Average bound alkyne per Co measured by ^1H NMR spectroscopy in benzene- d_6 versus $\text{Si}(\text{SiMe}_3)_4$ as an internal standard with the NMR probe temperature calibrated and set to 338 K.

While similar ligand substitution behavior was observed with (*N*-aryl)aryl ethanimine, productive C–H activation did not occur. Thus, stoichiometric treatment of **Co-Li** with imine **1a** in benzene- d_6 at 65 °C did not result in the generation of a new cyclometallated species after 2 d; instead, only broadened ^1H NMR resonances for **1a**, likely the result of rapid ligand exchange with PPh_3 , were observed.

Reactant Order and Catalytic Kinetics. The reaction profile with complex **Co-Li** as catalyst was monitored by ^1H NMR spectroscopy at 65 °C (Figure 2). Initial time points reveal that the *E*-isomer is the kinetic product; conversion to **Z-3a** occurred only after the formation of **E-3a**. These data are consistent with an off-cycle isomerization process to generate the *Z*-isomer as the thermodynamic product.

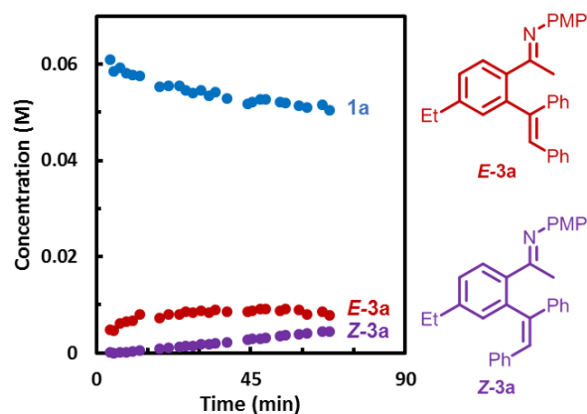


Figure 2. Representative initial reaction kinetic profile of the hydroarylation of **1a** ($[1a]_0 = 67$ mM) with diphenylacetylene ($[alkyne]_0 = 67$ mM) catalyzed by **Co-Li** ($[Co-Li]_0 = 2$ mM, 3 mol%). Reaction was monitored by 1H NMR spectroscopy in benzene- d_6 versus $Si(SiMe_3)_4$ as an internal standard with the NMR probe temperature calibrated and set to 339 K. See Supporting Information, Figure S18 for additional representative reaction profiles.

With **Co-Li** as the catalyst, an initial catalytic rate constant was calculated at 338 K to be $k_{obs} = 9(2) \times 10^{-4} s^{-1}$ (Figure 3A) with a first-order dependence on $[Co-Li]_0$ (Figure 3B). No observable difference in initial rate occurred when 12-crown-4 was added to the catalytic mixture. This result would seem to rule out participation of the Li counterion as a Lewis-acid in the catalysis. Significantly slower catalysis occurred with the bimetallic complex **Co₂-Mg** (Figure 4A), with a calculated catalytic rate constant of $k_{obs} = 3.0(3) \times 10^{-5} s^{-1}$ as measured at 339 K, which implicates slow decoordination of the active L_3Co^{-1} fragment from the Mg^{2+} counterion. Surprisingly, a first-order dependence on $[Co_2-Mg]_0$ (Figure 4B) suggests that only a single catalytically active Co fragment exists along with an inert $[L_3Co(N_2)]Mg^+$ counterion, which implicates Li^+ as the better dissociating counter cation.

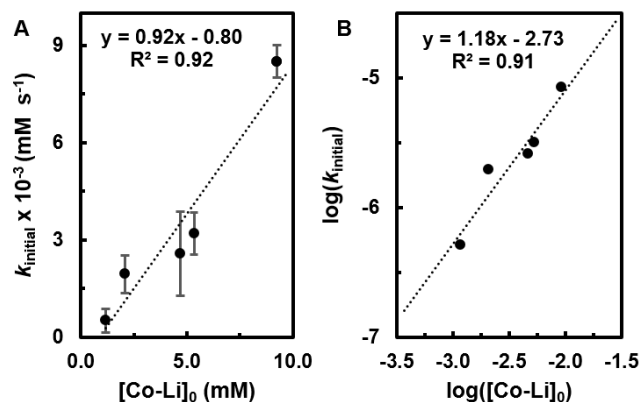


Figure 3. A: Dependence of $[Co-Li]_0$ on the hydroarylation of **1a** ($[1a]_0 = 67$ mM) with diphenylacetylene ($[alkyne]_0 = 67$ mM). Initial rates ($k_{initial}$) were determined by 1H NMR spectroscopy in benzene- d_6 vs $Si(SiMe_3)_4$ as an internal standard with the NMR probe temperature calibrated and set to 338 K. The dashed line is a linear fit of the data with a slope of $k_{obs} = 9(2) \times 10^{-4} s^{-1}$. Error of the fit

slope was determined as the standard error of the linear regression ($R^2 = 0.92$, $S_x = 1.6 \times 10^{-4} s^{-1}$). Error bars were determined from the standard deviation of triplicate experiments **B:** log-log plot depiction of the first-order dependence of $[Co-Li]_0$ on the initial rate (slope ~ 1). Error determined as the standard error of the linear regression ($R^2 = 0.91$, $S_x = 0.2$).

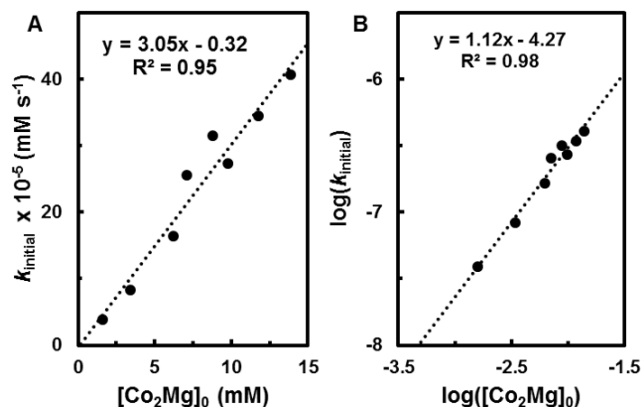


Figure 4. A: Dependence of $[Co_2-Mg]_0$ on the hydroarylation of **1a** ($[1a]_0 = 67$ mM) with diphenylacetylene ($[alkyne]_0 = 67$ mM). Initial rates ($k_{initial}$) were determined by 1H NMR spectroscopy in benzene- d_6 vs $Si(SiMe_3)_4$ as an internal standard with the NMR probe temperature calibrated and set to 339 K. The dashed line is a linear fit of the data with a slope of $k_{obs} = 3.0(3) \times 10^{-5} s^{-1}$. Error determined as the standard error of the linear regression ($R^2 = 0.95$, $S_x = 0.3 \times 10^{-5} s^{-1}$). **B:** log-log depiction of the first-order dependence of $[Co_2-Mg]_0$ on the initial rate (slope ca. 1.1). Error determined as the standard error of the linear regression ($R^2 = 0.98$, $S_x = 0.06$).

Each of the substrates displayed saturation-type kinetics, with pseudo-first order dependencies at low substrate concentrations. Given these results, a Michaelis-Menten analysis was used to further examine the catalytic mechanism. Typically, such studies are performed to elucidate the origin of saturation behavior, using various models for enzyme inhibition.^{72,73} By presenting the data in a Lineweaver-Burk double-reciprocal plot, two key mechanistic features can be extracted from a linear fit, namely the maximum achievable rate ($v_{max} = 1/\text{intercept}_y$) and a modified binding constant ($K_M = -1/\text{intercept}_x$). Three main classes of enzymatic inhibition mechanisms exist, which result from competitive (K_M increases), uncompetitive (both V_{max} and K_M decrease), and non-competitive (v_{max} decreases) binding of the inhibitor.⁷³

With these mechanistic factors in mind, an enzymatic-like kinetic analysis was applied to the cobalt-catalyzed hydroarylations described herein. The hydroarylations of diphenylacetylene with **1a** at various initial substrate concentrations were monitored by 1H NMR spectroscopy in benzene- d_6 at 338 K using complex **Co-Li** as the catalyst (7 mM; Figure 5). The initial catalytic rate constants ($k_{initial}$) were determined for each of these catalytic reactions (i.e., at each $[alkyne]_0$ and $[1a]_0$); at a fixed alkyne concentration, saturation-like imine dependence was observed and is reflected in a linear fit in the main double reciprocal plot. A series of such linear fits was generated at a variety of initial alkyne concentrations (see Supporting Information, Tables S13-S15). Each fit passed through the same y-

intercept from which an average v_{\max} was calculated to be $1.2(2) \times 10^{-5} \text{ M s}^{-1}$. Interestingly, the slope of each fit (K_M/v_{\max}) depends on the initial alkyne concentration, as illustrated in the expansion of Figure 5. This secondary Michaelis-Menten plot was fit to a hyperbolic function which contains a linear and an inverse dependence on alkyne concentration.

A model of the catalytic rate law was derived to account for the hyperbolic fit and the full derivation is described in the Supporting Information.⁷⁴ This Michaelis-Menten model (eq 6) relates the observed rate (v) to a function of the catalytic rate (where $v_{\max} = k_{\text{cat}}[\text{Co-Li}]_0$) and substrate binding equilibria

(where K_d and K_d' are the dissociation constants for **1a** and diphenylacetylene, respectively; K_a' is an off-cycle association constant). The observed alkyne kinetics result from the role of **1a** both as a substrate and a competitive inhibitor. That is, two discrete regimes exist: at low concentrations, the presence of alkyne increases the reaction rate, whereas high alkyne concentrations result in competitive inhibition, which is consistent with the formation of inactive bis(alkyne) off-cycle species. Indeed, precedent exists for such substrate inhibition, as observed in related Ir²⁸ and Ru⁷⁵ olefin hydroarylation systems.

$$\frac{1}{v} = \frac{1}{v_{\max}} + \frac{1}{v_{\max}[\mathbf{1a}]_0} \left(K_d + \frac{K_d'}{[\text{PhCCPh}]} + [\text{PhCCPh}]K_a' \right) \quad (6)$$

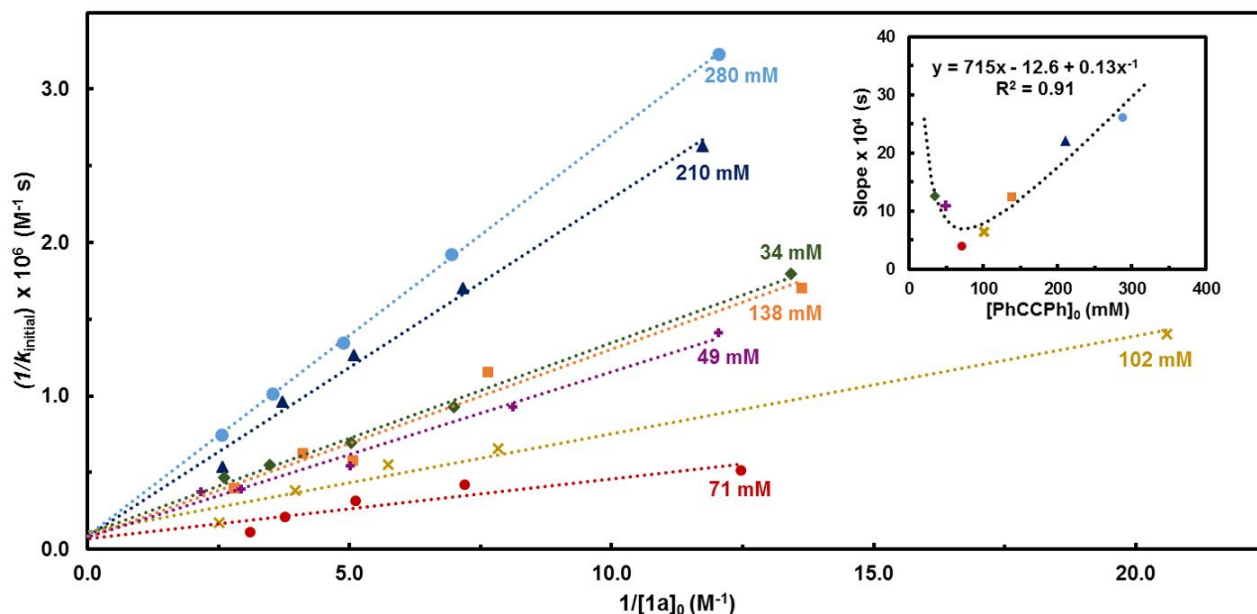


Figure 5. Lineweaver-Burk (double-reciprocal) plot of the hydroarylation of diphenylacetylene and **1a** catalyzed by **Co-Li** (7 mM). Initial rates (k_{initial}) were determined by ^1H NMR spectroscopy in benzene- d_6 with $\text{Si}(\text{SiMe}_3)_4$ as an internal standard with the NMR spectrometer probe calibrated and set to 338 K. Each experiment within a data set was performed at identical $[\text{diphenylacetylene}]_0$ as follows: **34 mM** (\bullet), **49 mM** ($+$), **71 mM** (\bullet), **102 mM** (\times), **138 mM** (\blacksquare), **210 mM** (\blacktriangle), and **280 mM** (\bullet). The colored dashed lines are the linear fits for each corresponding data set. Each fit has the same y-intercept which corresponds to a $v_{\max} = 1.2(2) \times 10^{-5} \text{ M s}^{-1}$. Error determined as the standard deviation of the average of y-intercepts from all 7 data sets. **Inset:** Plot of the slope of the linear fits from the main plot versus $[\text{diphenylacetylene}]_0$. The black dashed line represents a hyperbolic fit of the data.

Given the lability of the ancillary phosphine ligands under catalytic conditions, the influence of added PAr_3 on catalysis with **Co-Li** was investigated (Figure 6) with PPh_3 , PMes_3 and $\text{P}(\text{C}_6\text{F}_5)_3$. Surprisingly, additional PPh_3 promoted catalytic activity until saturation at ca. 50 equivs relative to **Co-Li**. A similar rate enhancement occurred with added PMes_3 , which gave saturation-like behavior at ca. 10 equivs relative to **Co-Li**. In contrast, the perfluorinated analogue, $\text{P}(\text{C}_6\text{F}_5)_3$, displayed a complex rate dependency; a modest rate increase was only observed at ca. 1-3 equiv of added $\text{P}(\text{C}_6\text{F}_5)_3$ relative to Co. It may be possible that added phosphine promotes the reaction rate either by stabilization of the active catalytic species or by changing the operative mechanism. Similar saturation behavior for ancillary ligands has been observed by Yoshikai and coworkers.³⁶ It is of note that C-H activation of the *ortho*-aryl position of PPh_3 does not occur (as determined by ^1H NMR spectroscopy), even at excess phosphine loadings.

Monitored catalysis by time-resolved $^{31}\text{P}\{^1\text{H}\}$ NMR spectroscopy probed the speciation of PPh_3 (Figure 7). Given the relatively low $[\text{PPh}_3]$ under catalytic conditions, a high-field NMR spectrometer equipped with a liquid N_2 cryoprobe broadband channel was used to facilitate direct observation of potential phosphorus-containing intermediates. Two new resonances were observed over the course of the catalysis (in addition to free PPh_3); the first at 69.27 ppm is attributed to a new, Co-bound PPh_3 ligand, given the similar shift for **Co-Li** (48.14 ppm). A second resonance at 9.90 ppm exists in a range similar to that of a phosphonium-ylide, which typically exhibits resonances between 5 to 20 ppm.⁷⁶ However, it is unclear whether this species might exist as a free “ylide” or is complexed by a Co fragment.⁷⁷⁻⁸³

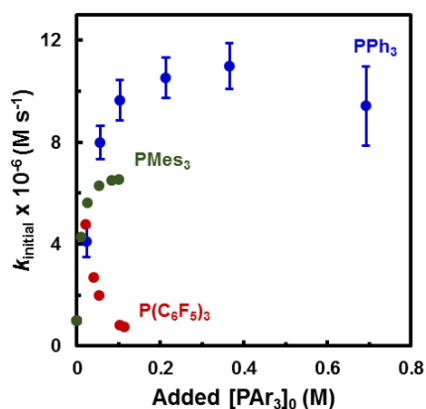


Figure 6. Dependence of added [PAR₃]₀ (PPh₃, PMes₃, or P(C₆F₅)₃) on the hydroarylation of **1a** ([**1a**]₀ = 67 mM) with diphenylacetylene ([alkyne]₀ = 67 mM) catalyzed by Co-Li ([Co-Li]₀ = 7 mM, 10 mol%). The reaction in benzene-*d*₆ was monitored by ¹H NMR spectroscopy versus Si(SiMe₃)₄ as an internal standard with the NMR probe temperature calibrated and set to 338 K. Error determined for reactions with added PPh₃ as the standard deviation of triplicate runs except at [PPh₃]₀ = 0.7 M, which was performed in pentaplicate.

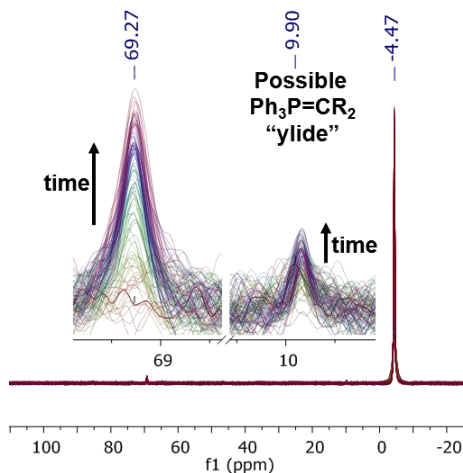


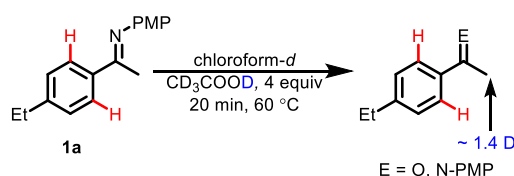
Figure 7. Time-resolved ³¹P{¹H} NMR spectra (benzene-*d*₆, 242.94 MHz) during the hydroarylation of **1a** ([**1a**]₀ = 67 mM) with diphenylacetylene ([alkyne]₀ = 67 mM) catalyzed by Co-Li ([Co-Li]₀ = 7 mM, 10 mol%). Spectra were acquired on a 600 MHz NMR spectrometer equipped with a liquid N₂ cryoprobe broadband channel with the NMR probe temperature calibrated to 339 K. All spectra over the course of the reaction are displayed atop one another as a stack. Time points were acquired every 20 s as the average of 8 scans (d1 = 1 s, d20 = 20 s, ns = 8). **Inset:** expansion of two new peaks observed at 69.27 and 9.90 ppm, which grow in over the course of the reaction. These peaks are attributed to a new bound PPh₃ complex and a phosphonium-ylide-like species, respectively.

Rate-Limiting C–H Activation and Isotope Effects. Deuteron-quenching experiments were utilized to probe the nature of the C–H activation step (Scheme 2). In a control experiment (Scheme 2A), a solution of imine **1a** in chloroform-*d* was treated with a slight excess of acetic acid-*d*₄ to afford a mixture

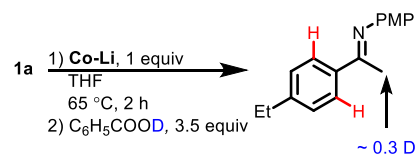
of *p*-anisidine, 4'-ethylacetophenone, and residual **1a**. Deuteron incorporation into the *ortho*-C–H bond was not observed; however, ca. 1.4 D was observed in the acetyl -C(O)CH₃ fragment of 4'-acetophenone and in the iminyl -C(N)CH₃ position of **1a**, which resulted from acid-catalyzed enol and enamine tautomerization, respectively. To probe the interaction of *ortho*-C–H bonds with the catalyst in the absence of alkyne, an equimolar mixture of **1a** and Co-Li in THF was heated to 65 °C for 2 h (Scheme 2B). Subsequent treatment with benzoic acid-*d* (C₆H₅COOD) afforded **1a** with D incorporation only in the iminyl fragment. An analogous experiment with equimolar quantities of **1a**, Co-Li, and diphenylacetylene (Scheme 2C) resulted in the formation of **Z/E-2a** and **Z/E-3a**. Interestingly, only acid-catalyzed exchange into the acetyl or iminyl groups occurred. That is, no *ortho*-H(D) exchange was observed. The existence of these hydroarylation products as well as the lack of *ortho*-deuterium incorporation in Scheme 2 suggest two possibilities. First, the C–H bond activation event may require the presence of alkyne to occur. Alternatively, the concentration of any intermediates derived from substrate deprotonation may not build up to an appreciable extent, thereby precluding interception by the added deuterium source.

Scheme 2. Stoichiometric Deuteron-Quenching Reactions.

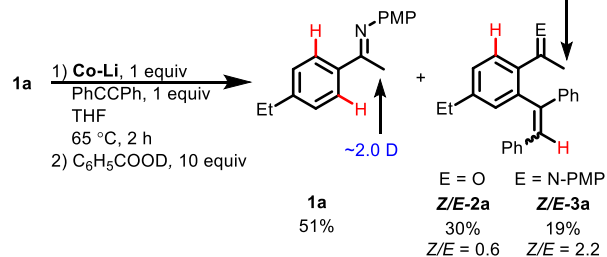
A) D⁺ Quench of **1a**, Control



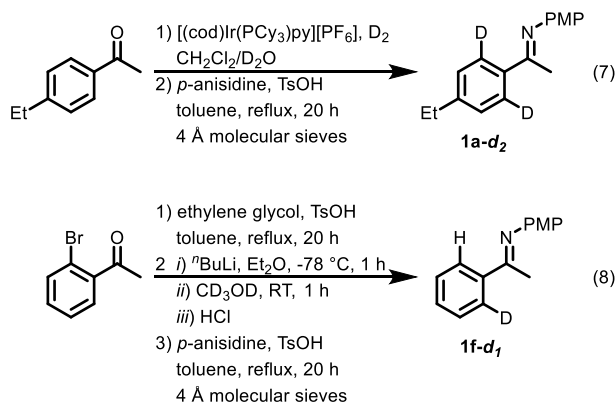
B) D⁺ Quench of **1a** and Co-Li, Control



C) D⁺ Quench of **1a**, Alkyne, and Co-Li

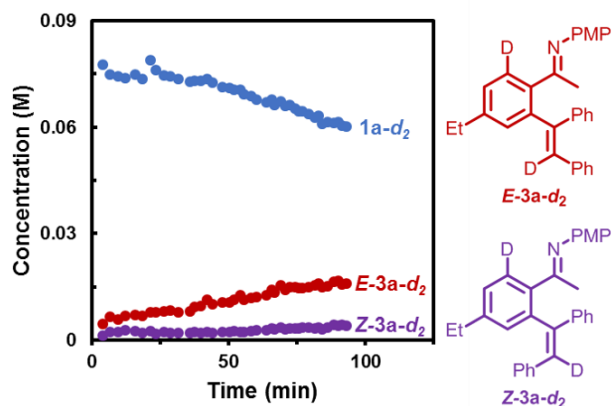


Further investigation of catalysis with isotopically enriched substrates probed the C–H activation step. *Ortho*-dideuterated imine **1a-d**₂ was synthesized by selective deuteration of 4'-ethylacetophenone with D₂ and Crabtree's catalyst followed by condensation with *p*-anisidine (eq 7). In addition, *ortho*-monodeuterated substrate **1f-d**₁ was synthesized from 2'-bromoacetophenone (eq 8).



13
14
15
16
17
18
19
20
21
22

Monitoring the hydroarylation of **1a-d₂** with **Co-Li** as the catalyst (14 mol%) by ¹H NMR spectroscopy provided an isotope effect on both the catalytic rate as well as the rate of isomerization (Figure 8). The replacement of C–H for C–D greatly diminished the observed rate of *Z*-olefin formation and implicates a C–H(D) cleavage step as being key to the isomerization. Analysis of the *Z/E*-**3a-d₂** products by ²H NMR spectroscopy confirmed deuterium incorporation into the vinylic position (6.60 ppm and 7.06 ppm, respectively) and retention of deuterium at the *ortho*-aryl position (7.86 ppm).



37
38
39
40
41
42

Figure 8. Representative initial reaction kinetic profile of the hydroarylation of **1a-d₂** ($[1a-d_2]_0 = 72$ mM) with diphenylacetylene ($[alkyne]_0 = 72$ mM) catalyzed by **Co-Li** ($[Co-Li]_0 = 10$ mM, 14 mol%). The reaction in benzene-*d*₆ was monitored by ¹H NMR spectroscopy versus Si(SiMe₃)₄ as an internal standard with the NMR probe temperature calibrated and set to 336 K.

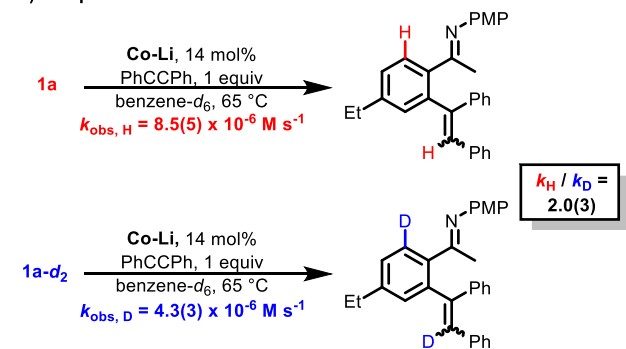
43
44
45
46
47
48
49
50
51
52
53
54
55

In separate reactions performed at identical concentrations of catalyst and substrates, the observed initial catalytic reaction rate constants $k_{H,obs}$ and $k_{D,obs}$ were determined to be $8.5(5) \times 10^{-6}$ M/s and $4.3(3) \times 10^{-6}$ M/s, respectively (Scheme 3A). The calculated KIE ($k_{H,obs}/k_{D,obs}$) of 2.0(3) is consistent with a rate-determining C–H cleavage.⁸⁴ Additional KIE experiments with equimolar amounts of **1a** and **1a-d₂** are consistent with this result; this intermolecular competition (Scheme 3B) resulted in an isotopic distribution corresponding to a KIE of 3.5, which is larger than that determined in the independent rate experiments due to differing reaction conditions; namely, the independent rates experiment employed benzene-*d*₆ as solvent, whereas the competition experiments used a mixture of

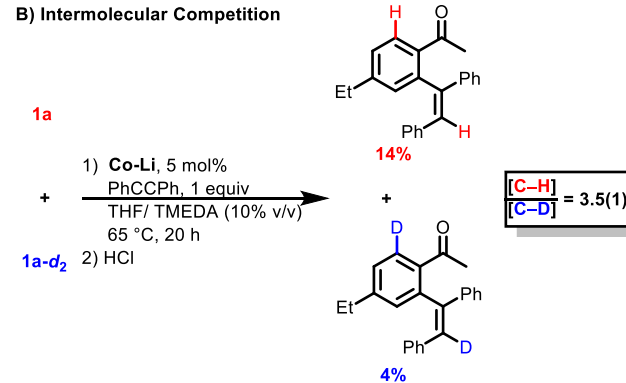
THF and TMEDA. The mixed products resulting from H(D)-crossover were not observed in this competition, which supports the C–H cleavage as a non-reversible step. Similarly, an intramolecular KIE was calculated to be 3.6 using imine **1f-d₁** bearing both an *ortho*-deuterium and *ortho*-proton (Scheme 3C).

Scheme 3. Kinetic Isotope Effect Studies.

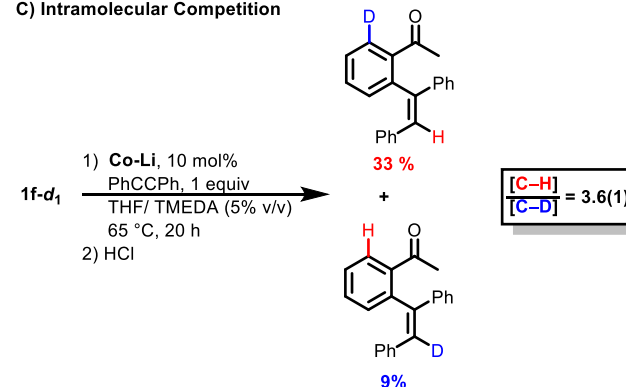
A) Independent Rate Determination



B) Intermolecular Competition



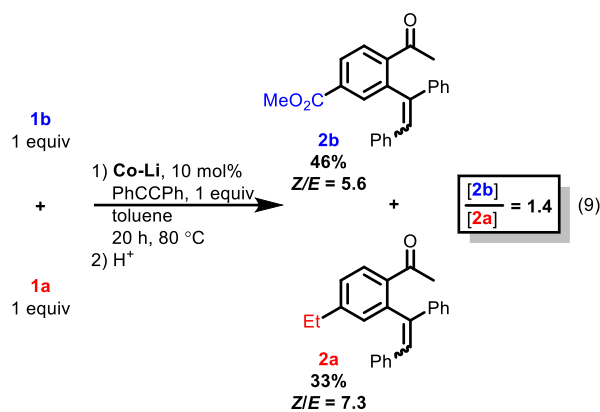
C) Intramolecular Competition



56
57
58
59
60

Substrate competition experiments further examined the nature of the C–H transfer step. In three separate experiments, equimolar amounts of electron rich and electron poor (*N*-aryl)aryl ethanimine substrates were subjected to catalytic conditions. The competition of **1a** and **1b** (eq 9) illustrates a representative trend that electron-poor arenes (e.g., CO₂Me) are favored over electron-rich substrates (e.g., Et) in the catalysis, which suggests that a proton-like transfer occurs in the C–H bond activation event.⁸⁵ Additional substrate competition

experiments are given in the Supporting Information (Figures S14-S17).



Independent rate measurements for the hydroarylations of the substituted (*N*-aryl)aryl ethanimines with Co-Li corroborated the competition experiments. The initial catalytic rates determined for 1a, 1b, 1d, and 1e appear to correlate with the σ_{para} and σ_{meta} parameters for the given substituent, as illustrated in the correlation plots (Figures 9A and 9C). The corresponding Hammett plots (Figures 9B and 9D) were generated by the normalization of the measured rates by the rate observed for 1a (k_X/k_{Et}). The electronic effects imparted by the substituent may affect any combination of three substrate-centered transformations (*i.e.*, imine pre-coordination and decoordination, and C–H activation). The *para*-parameter informs primarily on the imine coordination ability, whereas the *meta*-parameter influences the lability of C–H cleavage. The small, but positive slopes ($\rho'_{para} = 0.36(6)$ and $\rho'_{meta} = 0.6(2)$) of the normalized plot indicate that electron-withdrawing substituents may influence all of the aforementioned transformations. The weak correlation with the σ_{para} parameter indicates that electron-donating substituents dampen the observed initial rate compared to withdrawing functionalities, perhaps through prevention of competitive inhibition by additional imine donors. Interestingly, a stronger correlation exists with the σ_{meta} parameter, which suggests that the observed rate of catalysis may relate to the pK_a of the arene C–H bond. However, the relatively small rate enhancements observed in this series of substrates preclude the proposal of an unambiguous rationale.

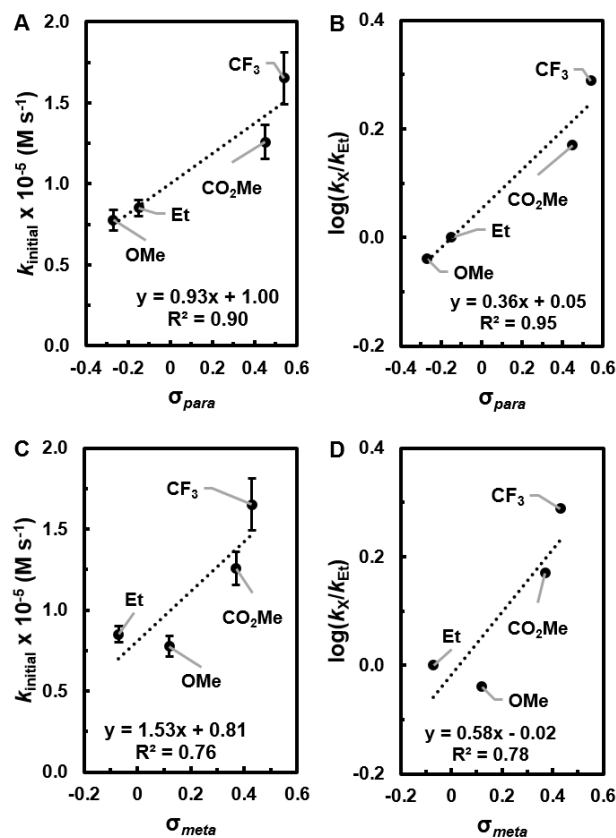


Figure 9. A: *para*-Hammett parameter (σ_{para}) versus the initial rate of hydroarylation for 1a (Et), 1b (CO₂Me), 1d (CF₃), and 1e (OMe). Catalytic conditions: (*N*-aryl)aryl ethanimine ($[1]_0 = 72$ mM) with diphenylacetylene ($[\text{PhCCPh}]_0 = 72$ mM) catalyzed by Co-Li ($[\text{Co-Li}]_0 = 10$ mM). The reactions in benzene-*d*₆ were monitored by ¹H NMR spectroscopy versus Si(SiMe₃)₄ as an internal standard with the NMR probe temperature calibrated to 340 K. Error bars determined as the standard deviation of triplicate runs. B: Normalized Hammett plot, which depicts the $\log(k_X/k_{Et})$ as a function of the Hammett parameter σ_{para} with a slope of $\rho'_{para} = 0.36(6)$, with error determined as the standard error of the linear regression ($R^2 = 0.95$, $S_x = 0.06$). C: *meta*-Hammett parameter (σ_{meta}) versus the initial rate of hydroarylation. D: Normalized Hammett plot, which depicts the $\log(k_X/k_{Et})$ as a function of the Hammett parameter σ_{meta} with a slope of $\rho'_{meta} = 0.6(2)$, with error determined as the standard deviation of the linear regression ($R^2 = 0.78$, $S_x = 0.22$).

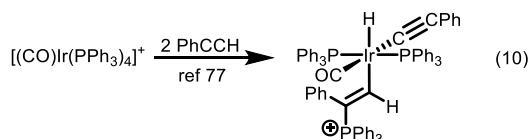
Proposed Mechanism for the Catalytic Cycle. Cumulatively, the results described above allow postulation of a reasonable mechanism for this catalysis (Scheme 4). The anionic complex Co-Li appears to be a direct precursor to the active catalytic species. Alkyne coordination occurs prior to the rate determining C–H activation step by displacement of PPh₃ and N₂ to generate the Co(alkyne) complex B which undergoes reversible imine precoordination to form complex C. It is also possible that multiple, non-productive alkyne ligation steps occur to form off-cycle species such as D. This type of complex is apparently not catalytically active based on the observed competitive inhibition described in the Michaelis-Menten study (Figure

5). Presumably, such complexes possess less activated alkyne ligands due to competitive π -backbonding.

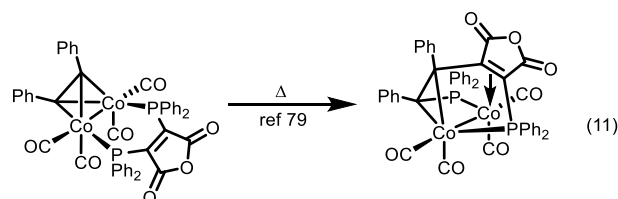
In catalytically productive steps, complex **C** may undergo C–H bond activation. One possible pathway (dashed) involves an intramolecular aryl C–H oxidative addition (OA) in **C** to afford a hydrido-Co(I) intermediate **E**; subsequent hydride insertion affords a (C,N)-chelated complex **F** bearing a diphenylvinyl fragment. Alternatively, a direct CMD-like mechanism may occur through a transition state akin to **TS^{C-F}**. Reductive elimination and substrate coordination afford the hydroarylation product as the *E*-isomer and regenerates **B**. However, these two mechanisms do not explain the rate enhancement observed with added PPh_3 .

An alternative C–H bond activation route (bold) involves an initial nucleophilic attack of exogenous PPh_3 onto the bound alkyne in **C** to afford the zwitterionic intermediate **G**. This species may be described by resonance structures involving charge localization on the alkyne β -carbon (**G₁**), the Co metal center (**G₂**), or across the entire alkyne. If addition of L to the cobalt center occurs instead at **C** or **G**, the resultant coordinatively saturated 18 e^- species would lack a requisite open coordination site for the H transfer step to occur. This should lead to a rate inhibition and not the observed rate enhancement.

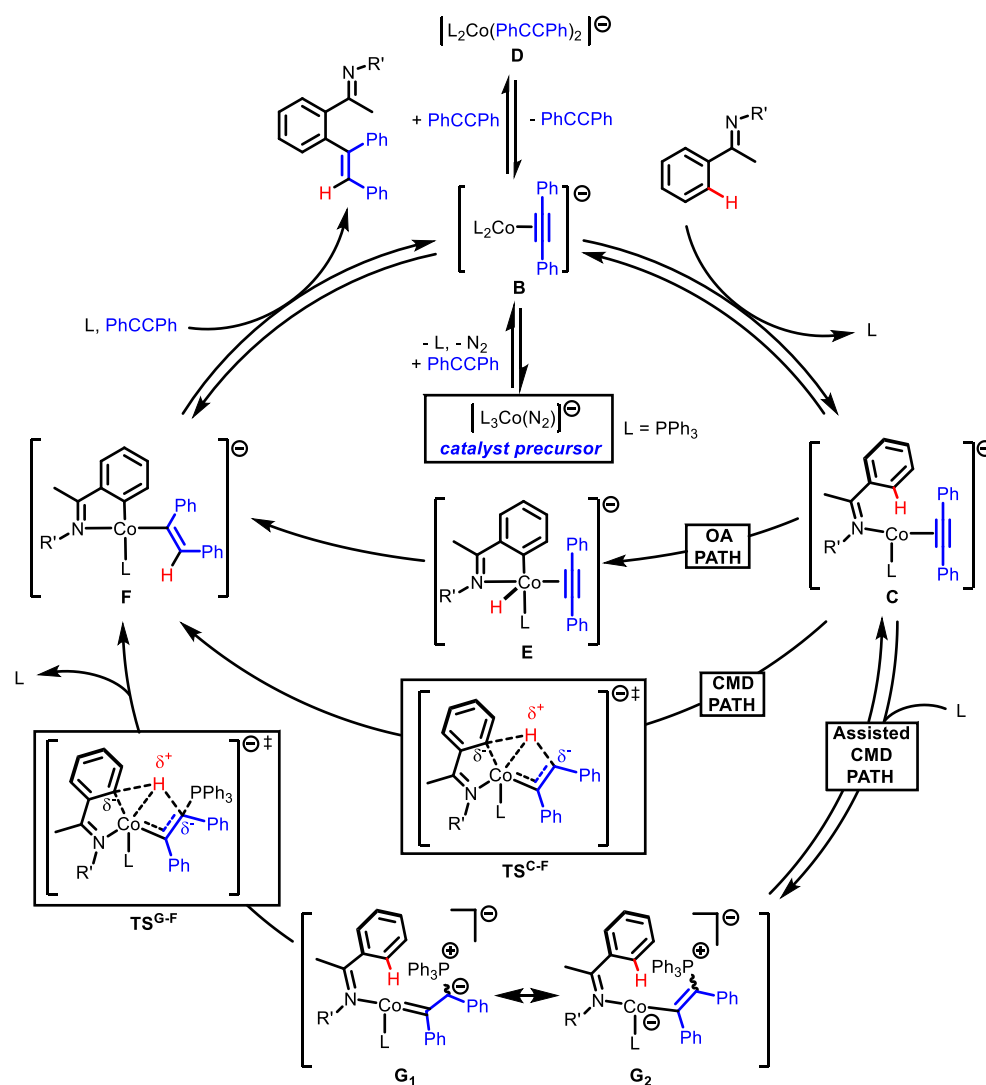
Indeed, precedent exists for phosphine addition to metal bound alkyne complexes.^{77–83} One example reported by Chin and coworkers⁷⁷ demonstrated that such additions occur upon exposure of $[(\text{CO})\text{Ir}(\text{PPh}_3)_4]^+$ to phenylacetylene (eq 10). The resultant metalo-phosponium-ylide complex exhibits a ^{31}P NMR resonance at 20.11 ppm (chloroform-*d*), which is similar to that observed for the Co intermediate described above (9.90 ppm, benzene-*d*₆, Figure 7).



An example of a first-row transition metal complex which undergoes phosphine assisted alkyne insertion was described by Huggins and Bergman.⁷⁸ In this report, $(\text{acac})\text{Ni}(\text{PPh}_3)\text{R}$ complexes were observed to react with internal alkynes of the type $\text{R}'\text{CCR}''$ to afford $(\text{acac})\text{Ni}(\text{CR}'=\text{CR}''\text{R})(\text{PPh}_3)$ species with an unusual distribution of *syn*- and *anti*-insertion products. They postulated that PPh_3 played a role in both the insertion process and off-cycle isomerizations by direct attack on $\text{Ni}(\text{alkyne})$ or $\text{Ni}(\text{vinyl})$ intermediates. While analogous reactivity with monometallic cobalt complexes has yet to be described, a bimetallic $\text{Co}_2(\text{alkyne})$ complex undergoes an intramolecular rearrangement to generate a new $\text{P}-\text{C}_{\text{alkyne}}$ bond (eq 11) that is reminiscent of a formal insertion (^{31}P resonances observed at 31.3 and 4.7 ppm in dichloromethane).⁷⁹ Phosphine-alkyne couplings have also been reported for Mo ,⁸⁰ Re ,⁸¹ Pd ,⁸² and Rh/Os heterobimetallic⁸³ complexes.



We propose that PPh_3 imparts Wittig-like character (and nucleophilicity) to the Co-bound carbon, as illustrated by resonance structure **G₁**, and thereby accesses a more facile C–H cleavage through a direct, H^+ transfer to afford **F** (via **TS^{G-F}**). Indeed, concerted metalation deprotonation (CMD) mechanisms have considerable theoretical precedence^{4,6,85–87} and have been invoked in the context of hydroarylation, specifically towards relevant arene-to-alkyne or arene-to-olefin H-transfer steps.^{39,40,57,88–90} Indeed, nucleophile assisted CMD mechanisms are invoked in several C–H activation processes, such as carboxylate-assisted thiophene activations with Pd ⁸⁵ or intramolecular cyclometallations of Grubbs-type complexes.⁹¹

Scheme 4. Proposed Mechanism for Alkyne Hydroarylation Catalyzed by Co-Li.^a

^a Counter-cations have been omitted for clarity.

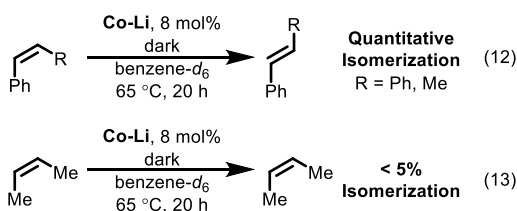
A related, low-valent cobalt system described by the Petit group⁵⁷ employed $(\text{PMe}_3)_4\text{Co}$ as the precatalyst and microwave conditions for alkyne hydroarylation. For this system, it was postulated that multiple phosphine dissociations occur to generate a monophosphine $\text{Co}(\text{PMe}_3)$ intermediates. On the basis of this assumption, computational studies indicated that a direct, ligand-to-ligand hydride transfer (similar to $\text{TS}^{\text{C-F}}$, Scheme 4) could account for the C–H activation event for this system.⁵⁷ The barrier for this concerted H-transfer was calculated to be $\Delta G^\ddagger = 15.9 \text{ kcal mol}^{-1}$ for the transition state corresponding to a $\text{Co}(0)$ center bearing imine, alkyne, and PMe_3 ligands. However, the Petit⁵⁷ mechanism does not include potential phosphine assistance.

The CMD mechanism^{4,6,85-87} is now well recognized as an important class of bond activation steps, and it seems likely that the hydroarylation catalysis with Co-Li involves such a C–H ac-

tivation pathway. In this context, we favor the phosphine-assisted CMD-like mechanism (bottom) over the classical oxidative bond cleavage path (top) or direct CMD path (middle).

Origin of Observed Olefin Z/E-Selectivity: Off-Cycle Isomerization. To investigate the off-cycle isomerization process, a series of disubstituted olefins was treated with catalytic quantities of complex Co-Li in the dark to avoid adventitious photoisomerization (eqs 12 and 13). Quantitative isomerization occurred after 20 h at 65 °C for mono- or diaryl substituted *cis*-olefins (i.e., *cis*-stilbene and *cis*- β -methylstyrene, eq 12) to afford the corresponding *trans*-olefin; surprisingly, complex Co-Li was unreactive towards dialkyl olefins (i.e., *cis*-2-butene, eq 13). Upon stoichiometric addition of a hydrogen-atom source (i.e., 9,10-dihydroanthracene, DHA), *cis*-2-butene was converted to *trans*-2-butene with a half-life of ca. 5 h at 65 °C (quantitative after 20 h). The reverse isomerization (i.e., *trans*-to *cis*-) did not occur to an appreciable extent; after 20 h at 65

°C with added **Co-Li**, *trans*-stilbene remained stereometrically pure.



The kinetic profiles of the isomerization process with *cis*-stilbene (Figure 10A) and *cis*- β -methylstyrene (Figure 11A) as the substrates were investigated by ^1H NMR spectroscopy in benzene- d_6 at 22 °C. The dependence of the isomerization rate on [olefin] revealed a first-order rate dependence for the case of *cis*-stilbene (Figure 10B; $k_{\text{obs}} = 3.1(2) \times 10^{-6} \text{ s}^{-1}$), but an inverse first-order dependence for *cis*- β -methylstyrene (Figure 11B; $k_{\text{obs}} = 1.3(1) \times 10^{-7} \text{ M}^{-1} \text{ s}^{-1}$). After ca. 3 days at 22 °C, near quantitative conversion ($\sim 95\%$) to the *trans*-isomer was observed for both olefin substrates.

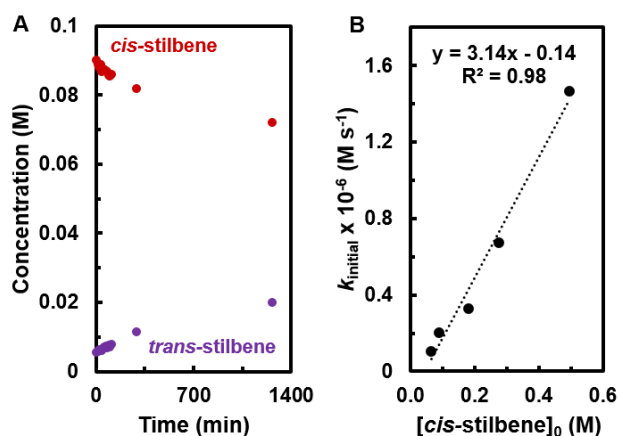


Figure 10. **A:** Representative kinetic profile of *cis*-stilbene ($[\textit{cis}\text{-stilbene}]_0 = 95 \text{ mM}$) isomerization catalyzed by **Co-Li** (10 mol%, $[\text{Co-Li}]_0 = 7 \text{ mM}$) as determined by ^1H NMR spectroscopy in benzene- d_6 vs $\text{Si}(\text{SiMe}_3)_4$ as an internal standard with the NMR probe temperature calibrated and set to 295 K. **B:** Dependence of isomerization rate on $[\textit{cis}\text{-stilbene}]_0$. The dashed line is a linear fit of the data with a slope of $k_{\text{obs}} = 3.1(2) \times 10^{-6} \text{ s}^{-1}$. Error determined as the standard error of the linear regression ($R^2 = 0.98$, $S_x = 0.2 \times 10^{-6} \text{ s}^{-1}$).

Cobalt-catalyzed olefin isomerizations have recently been reported by Hilt and coworkers.⁹² Isomerization of terminal olefins of the type $\text{H}_2\text{C}=\text{CHCH}_2\text{R}$ into a mixture of *E*- and *Z*-internal olefins was observed upon treatment with a mixture of $\text{CoBr}_2(\text{PR}_3)_2$, Zn, ZnI_2 , and Ph_2PH . Isomerization required the use of Ph_2PH , presumably because the key mechanistic step involves reversible H-transfer to the olefin to generate the cobalt intermediate $\text{L}_2\text{Co}(\text{H}_3\text{C}-\text{CHCH}_2\text{R})(=\text{PPh}_2)$. Free rotation about the previously olefinic C–C bond in the resultant saturated alkyl fragment may occur, which results in formation of the observed mixture of *E*- and *Z*-olefin products. In contrast to the system described by Hilt,⁹² complex **Co-Li** isomerizes internal

diarylolefins without the addition of a reagent that might produce a cobalt hydride species. However, it seems likely that a Co–H species, formed under the reaction conditions, may be responsible for the observed isomerization.

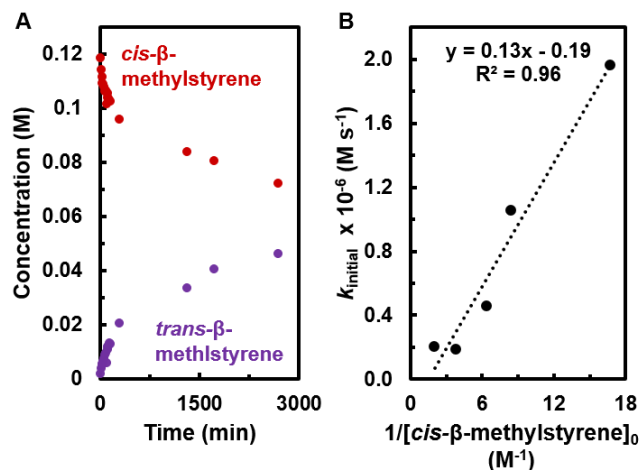


Figure 11. **A:** Representative kinetic profile of *cis*- β -methylstyrene ($[\textit{cis}\text{-}\beta\text{-methylstyrene}]_0 = 120 \text{ mM}$) isomerization catalyzed by **Co-Li** (10 mol%, $[\text{Co-Li}]_0 = 7 \text{ mM}$) as determined by ^1H NMR spectroscopy in benzene- d_6 vs $\text{Si}(\text{SiMe}_3)_4$ as an internal standard with the NMR probe temperature calibrated and set to 295 K. **B:** Dependence of isomerization rate on $[\textit{cis}\text{-}\beta\text{-methylstyrene}]_0$. The dashed line is a linear fit of the data with a slope of $k_{\text{obs}} = 1.3(1) \times 10^{-7} \text{ M}^{-1} \text{ s}^{-1}$. Error determined as the standard error of the linear regression ($R^2 = 0.96$, $S_x = 0.1 \times 10^{-7} \text{ M}^{-1} \text{ s}^{-1}$).

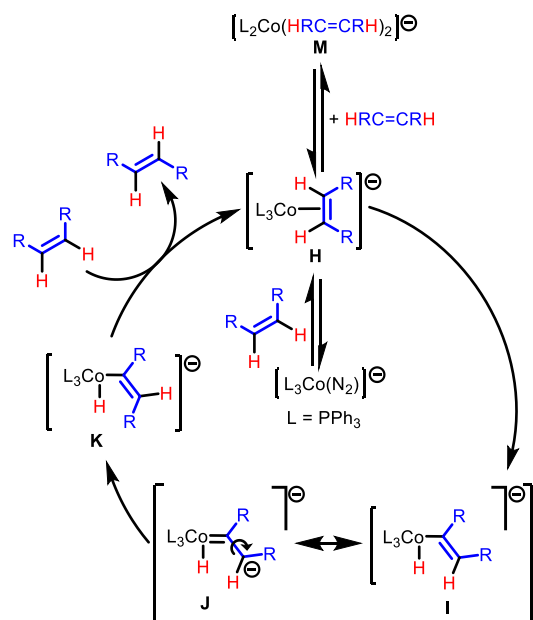
These results point to a catalytic, off-cycle isomerization event that accounts for the observed *Z*-selectivity in the hydroarylation process (Scheme 5). Initial coordination of *cis*-olefin to complex **Co-Li** occurs to give intermediate **H**. A formal C–H oxidative addition of the bound olefin of **H** could produce the hydride species **I** bearing a *cis*-vinyl fragment. Cobalt-vinyl intermediates such as **F** (Scheme 4) and **I** (Scheme 5), may undergo olefin isomerization in a manner similar to that postulated by Huggins and Bergman⁷⁸ for analogous *trans*-isomerization in vinylic complexes derived from *cis*-insertions of aryl-substituted alkynes into a Ni–H bond. It was posited by these authors⁷⁸ that such Ni-based alkyne complexes exhibit charge localization on the diaryl-vinyl ligand, thereby reducing the double-bond character and allowing C–C bond rotation. Indeed, a related group 9 species, $[\text{Cp}^*\text{Rh}(\text{CPh}=\text{CHPh})(\text{PMe}_3)]^+$, undergoes this vinyl isomerization process through such a mechanism.⁹³

Anionic character in the analogous Co–vinyl complex **I** should concentrate negative charge on the benzylic β -C as indicated in resonance structure **J**, which is stabilized in the presence of aryl substituents (e.g., R = Ph). This aryl-group resonance stabilization of a carbanionic center would account for the observation that *cis*-stilbene and *cis*- β -methylstyrene are rapidly isomerized by **Co-Li**, whereas *cis*-2-butene is unreactive under comparable conditions. A low-energy C–C bond rotation in **J** would result in formation of a cobalt-bound *trans*-vinyl ligand (**K**). Reductive elimination and ligand substitution would

then liberate the observed *trans*-olefin and regenerate **H**. It is possible that PPh₃ addition (akin to intermediate **G** proposed above in Scheme 4) may play a role in the observed isomerization process.

It is plausible that a second olefin may bind to **H** to form the bis(olefin) complex **M**, which may be catalytically incompetent. It is likely that olefin size may suppress the formation of such off-cycle species, which is consistent with observation of the first-order dependence on *cis*-stilbene and inverse first-order dependence on *cis*- β -methylstyrene.

Scheme 5. Proposed Olefin Isomerization Mechanism. ^a



^a Counter-cations have been omitted for clarity.

The apparent lack of appreciable isomerization in the Yoshikai system³⁶ may implicate alternative isomerization pathways that are operative with different initiation reagents. For example, activation of CoBr₂ with the Grignard reagents ^tBuCH₂MgX or Me₃SiCH₂MgX may result in reduction to a Co(0) species as the active catalyst. Such species may not be as active for olefin isomerization as **Co-Li**, as illustrated by the observation of primarily *E*-isomers in the Yoshikai system.³⁶

CONCLUSIONS

Significantly, this mechanistic study has developed a highly reduced, single-component cobalt catalyst for alkyne hydroarylations. Initiation of catalysis occurs via a three-step pathway (i.e., transmetalation, β -H elimination, deprotonation) to afford a dinitrogen Co(I) complex, **Co-Li**. Evidence for the catalytic mechanism, such as the moderate primary isotope effect and the observed requirement that alkyne binds prior to the C–H activation, implicates a CMD mechanism.^{4,6,39,40,57,88,89} Modified Michaelis-Menten enzyme kinetic analysis revealed a complex dependency of the substrates on the observed reaction rate; while both substrates display saturation-like kinetics, competitive substrate inhibition occurs at non-equimolar concentrations of (*N*-aryl)aryl ethanimine and

alkyne. This may be a result of an additional alkyne coordination to formation of an off-cycle bis(alkyne) complex. Interestingly, rate enhancements were observed with additional ancillary ligand, which implicates PAR₃ as a non-innocent reactant in this system. The observed *Z*-selectivity occurs by an off-cycle olefin isomerization catalyzed by **Co-Li**. Interestingly, only aryl-substituted olefins (i.e., stilbene, β -methylstyrene) undergo *cis*-to-*trans* isomerization, which may implicate free rotation about the C–C bond within a metallo-carbanion intermediate.

These mechanistic insights should prove useful in the design of new first row transition metal catalysts that utilize C–H activations and C–C bond hydroarylations. In particular, the identity of the active species and the mechanism of initiation provide insight into structural requirements for competent catalysis. Highly reduced species exhibit catalytic activity, and such species appear to be generated *in situ* when cobalt dihalide species are activated with organometallic reagents (e.g., RMgBr, RLi, AlR₃, etc.). This information provides concepts for developing first row-metal, single-component catalysts that are storable in solid-state, which circumvents the need for multiple, solution-state reagents.

ASSOCIATED CONTENT

Supporting Information

Experimental details, characterization data, kinetics data, and rate law derivation are found in the Supporting Information and are available free of charge via the Internet at <http://pubs.acs.org>.

AUTHOR INFORMATION

Corresponding Author

* E-mail: tdtilley@berkeley.edu

ORCID

Benjamin A. Suslick: 0000-0002-6499-3625

T. Don Tilley: 0000-0002-6671-9099

Notes

The authors declare no competing financial interests.

ACKNOWLEDGMENT

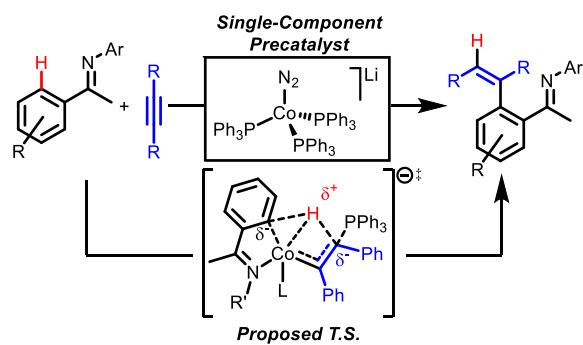
This work was primarily funded by the U.S. Department of Energy, Office of Science, Office of Basic Energy Sciences, Chemical Sciences, Geosciences, and Biosciences Division under Contract No. DE-AC02-05CH11231. We acknowledge the NIH (Grant Nos. *SRR023679A*, *1S10RR016634-01*, *S10OD024998*) and NSF (Grant No. *CHE-0130862*) for funding of the College of Chemistry NMR facility (University of California, Berkeley). The QB3/Chemistry Mass Spectrometry Facility (University of California, Berkeley) is acknowledged for help and access to the LTQ-FT ESI-HRMS (SN 06053F) and AutoSpec EI-HRMS (SN P749, property ID#20081000740) instruments. Dr. Hasan Celik is thanked for help with high-field, variable temperature NMR spectroscopy experiments. B.A.S. acknowledges the NSF-GRFP for a fellowship (DGE 1106400). Professor Robert G. Bergman, Dr. Ryan Witzke, Dr. Patrick Smith, Dr. Gavin Kiel, Rex Handford, Harrison Bergman, Dr. Addison Desnoyer, Dr. D. Dawson Beattie, and T. Alex Wheeler are thanked for providing useful discussions and insights. James Breen is thanked for copious glassware repairs and fabrications.

REFERENCES

- (1) Wang, S.; Chen, S. Y.; Yu, X. Q. C-H Functionalization by High-Valent Cp*Co(III) Catalysis. *Chem. Commun.* **2017**, *53*, 3165-3180.
- (2) Moselage, M.; Li, J.; Ackermann, L. Cobalt-Catalyzed C-H Activation. *ACS Catal.* **2016**, *6*, 498-525.
- (3) Gao, K.; Yoshikai, N. Low-Valent Cobalt Catalysis: New Opportunities for C-H Functionalization. *Acc. Chem. Res.* **2014**, *47*, 1208-1219.
- (4) Vastine, B. A.; Hall, M. B. Carbon-Hydrogen Bond Activation: Two, Three, or More Mechanisms? *J. Am. Chem. Soc.* **2007**, *129*, 12068-12069.
- (5) Pototschnig, G.; Maulide, N.; Schnürch, M. Direct Functionalization of C-H Bonds by Iron, Nickel, and Cobalt Catalysis. *Chem. Eur. J.* **2017**, *23*, 9206-9232.
- (6) Balcells, D.; Clot, E.; Eisenstein, O. C-H Bond Activation in Transition Metal Species from a Computational Perspective. *Chem. Rev.* **2010**, *110*, 749-823.
- (7) Lersch, M.; Tilset, M. Mechanistic Aspects of C-H Activation by Pt Complexes. *Chem. Rev.* **2005**, *105*, 2471-2526.
- (8) Colby, D. A.; Bergman, R. G.; Ellman, J. A. Rhodium-Catalyzed C-C Bond Formation Via Heteroatom-Directed C-H Bond Activation. *Chem. Rev.* **2010**, *110*, 624-655.
- (9) Suslick, B. A.; Tilley, T. D. Hydroarylation of Olefins with Complexes Bearing d⁸ Metal Centers in *Catalytic Hydroarylation of Carbon-Carbon Multiple Bonds*; Ackermann, L., Gunnoe, T. B., Habgood, L. G., Eds.; Wiley-VCH: Weinheim, 2017, p 107-174.
- (10) Evano, G.; Theunissen, C. Beyond Friedel and Crafts: Innate Alkylation of C-H Bonds in Arenes. *Angew. Chem. Int. Ed.* **2019**, *58*, 7558-7598.
- (11) Murai, S.; Kakiuchi, F.; Sekine, S.; Tanaka, Y.; Kamatani, A.; Sonoda, M.; Chatani, N. Efficient Catalytic Addition of Aromatic Carbon-Hydrogen Bonds to Olefins. *Nature* **1993**, *366*, 529.
- (12) Kakiuchi, F.; Murai, S. Catalytic C-H/Olefin Coupling. *Acc. Chem. Res.* **2002**, *35*, 826-834.
- (13) Thalji, R. K.; Ahrendt, K. A.; Bergman, R. G.; Ellman, J. A. Annulation of Aromatic Imines Via Directed C-H Activation with Wilkinson's Catalyst. *J. Am. Chem. Soc.* **2001**, *123*, 9692-9693.
- (14) Ryu, J.; Cho, S. H.; Chang, S. A Versatile Rhodium(I) Catalyst System for the Addition of Heteroarenes to Both Alkenes and Alkynes by a C-H Bond Activation. *Angew. Chem. Int. Ed.* **2012**, *51*, 3677-3681.
- (15) Lim, S.-G.; Ahn, J.-A.; Jun, C.-H. Ortho Alkylation of Aromatic Ketimine with Functionalized Alkene by Rh(I) Catalyst. *Org. Lett.* **2004**, *6*, 4687-4690.
- (16) Jun, C. H.; Hong, J. B.; Kim, Y. H.; Chung, K. Y. The Catalytic Alkylation of Aromatic Imines by Wilkinson's Complex: The Domino Reaction of Hydroacylation and Ortho-Alkylation. *Angew. Chem. Int. Ed.* **2000**, *39*, 3440-3442.
- (17) Webster-Gardiner, M. S.; Fu, R.; Fortman, G. C.; Nielsen, R. J.; Gunnoe, T. B.; Goddard III, W. A. Arene C-H Activation Using Rh(I) Catalysts Supported by Bidentate Nitrogen Chelates. *Catalysis Science & Technology* **2015**, *5*, 96-100.
- (18) Yamaguchi, T.; Natsui, S.; Shibata, K.; Yamazaki, K.; Rej, S.; Ano, Y.; Chatani, N. Rhodium-Catalyzed Alkylation of C-H Bonds in Aromatic Amides with Non-Activated 1-Alkenes: The Possible Generation of Carbene Intermediates from Alkenes. *Chem. Eur. J.* **2019**, *25*, 6915-6919.
- (19) Sevov, C. S.; Hartwig, J. F. Iridium-Catalyzed Intermolecular Asymmetric Hydroheteroarylation of Bicycloalkenes. *J. Am. Chem. Soc.* **2013**, *135*, 2116-2119.
- (20) Ebe, Y.; Nishimura, T. Iridium-Catalyzed Branch-Selective Hydroarylation of Vinyl Ethers Via C-H Bond Activation. *J. Am. Chem. Soc.* **2015**, *137*, 5899-5902.
- (21) Crisenza, G. E. M.; McCreanor, N. G.; Bower, J. F. Branch-Selective, Iridium-Catalyzed Hydroarylation of Monosubstituted Alkenes Via a Cooperative Destabilization Strategy. *J. Am. Chem. Soc.* **2014**, *136*, 10258-10261.
- (22) Matsumoto, T.; Taube, D. J.; Periana, R. A.; Taube, H.; Yoshida, H. Anti-Markovnikov Olefin Arylation Catalyzed by an Iridium Complex. *J. Am. Chem. Soc.* **2000**, *122*, 7414-7415.
- (23) Periana, R. A.; Liu, X. Y.; Bhalla, G. Novel Bis-Acac-O₂-Ir(III) Catalyst for Anti-Markovnikov, Hydroarylation of Olefins Operates by Arene C-H Activation. *Chem. Commun.* **2002**, 3000-3001.
- (24) Oxgaard, J.; Muller, R. P.; Goddard, W. A.; Periana, R. A. Mechanism of Homogeneous Ir(III) Catalyzed Regioselective Arylation of Olefins. *J. Am. Chem. Soc.* **2004**, *126*, 352-363.
- (25) Oxgaard, J.; Periana, R. A.; Goddard, W. A. Mechanistic Analysis of Hydroarylation Catalysts. *J. Am. Chem. Soc.* **2004**, *126*, 11658-11665.
- (26) Bhalla, G.; Oxgaard, J.; Goddard, W. A.; Periana, R. A. Anti-Markovnikov Hydroarylation of Unactivated Olefins Catalyzed by a Bis-Tropolonato Iridium(III) Organometallic Complex. *Organometallics* **2005**, *24*, 3229-3232.
- (27) Bhalla, G.; Bischof, S. M.; Ganesh, S. K.; Liu, X. Y.; Jones, C. J.; Borzenko, A.; Tenn, I. I. W. J.; Ess, D. H.; Hashiguchi, B. G.; Lokare, K. S.; Leung, C. H.; Oxgaard, J.; Goddard, I. I. W. A.; Periana, R. A. Mechanism of Efficient Anti-Markovnikov Olefin Hydroarylation Catalyzed by Homogeneous Ir(III) Complexes. *Green Chem.* **2011**, *13*, 69-81.
- (28) Matsumoto, T.; Periana, R. A.; Taube, D. J.; Yoshida, H. Regioselective Hydrophenylation of Olefins Catalyzed by an Ir(III) Complex. *J. Mol. Catal. A: Chem.* **2002**, *180*, 1-18.
- (29) Podhajsky, S. M.; Iwai, Y.; Cook-Sneathen, A.; Sigman, M. S. Asymmetric Palladium-Catalyzed Hydroarylation of Styrenes and Dienes. *Tetrahedron* **2011**, *67*, 4435-4441.
- (30) Suslick, B. A.; Liberman-Martin, A. L.; Wambach, T. C.; Tilley, T. D. Olefin Hydroarylation Catalyzed by (Pyridyl-Indolate)Pt(II) Complexes: Catalytic Efficiencies and Mechanistic Aspects. *ACS Catal.* **2017**, *7*, 4313-4322.
- (31) McKeown, B. A.; Gonzalez, H. E.; Friedfeld, M. R.; Gunnoe, T. B.; Cundari, T. R.; Sabat, M. Mechanistic Studies of Ethylene Hydrophenylation Catalyzed by Bipyridyl Pt(II) Complexes. *J. Am. Chem. Soc.* **2011**, *133*, 19131-19152.
- (32) Luedtke, A. T.; Goldberg, K. I. Intermolecular Hydroarylation of Unactivated Olefins Catalyzed by Homogeneous Platinum Complexes. *Angew. Chem. Int. Ed.* **2008**, *47*, 7694-7696.
- (33) Vaughan, B. A.; Khani, S. K.; Gary, J. B.; Kammert, J. D.; Webster-Gardiner, M. S.; McKeown, B. A.; Davis, R. J.; Cundari, T. R.; Gunnoe, T. B. Mechanistic Studies of Single-Step Styrene Production Using a Rhodium(I) Catalyst. *J. Am. Chem. Soc.* **2017**, *139*, 1485-1498.
- (34) Chirik, P.; Morris, R. Getting Down to Earth: The Renaissance of Catalysis with Abundant Metals. *Acc. Chem. Res.* **2015**, *48*, 2495.
- (35) Kimura, N.; Kochi, T.; Kakiuchi, F. Iron-Catalyzed Regioselective Anti-Markovnikov Addition of C-H Bonds in Aromatic Ketones to Alkenes. *J. Am. Chem. Soc.* **2017**, *139*, 14849-14852.
- (36) Lee, P.-S.; Fujita, T.; Yoshikai, N. Cobalt-Catalyzed, Room-Temperature Addition of Aromatic Imines to Alkynes Via Directed C-H Bond Activation. *J. Am. Chem. Soc.* **2011**, *133*, 17283-17295.
- (37) Bera, S.; Hu, X. Nickel-Catalyzed Regioselective Hydroalkylation and Hydroarylation of Alkenyl Boronic Esters. *Angew. Chem. Int. Ed.* **2019**, *58*, 13854-13859.

- (38) Barber, E. R.; Hynds, H. M.; Stephens, C. P.; Lemons, H. E.; Fredrickson, E. T.; Wilger, D. J. Nickel-Catalyzed Hydroarylation of Alkynes under Reductive Conditions with Aryl Bromides and Water. *J. Org. Chem.* **2019**, *84*, 11612–11622.
- (39) Bair, J. S.; Schramm, Y.; Sergeev, A. G.; Clot, E.; Eisenstein, O.; Hartwig, J. F. Linear-Selective Hydroarylation of Unactivated Terminal and Internal Olefins with Trifluoromethyl-Substituted Arenes. *J. Am. Chem. Soc.* **2014**, *136*, 13098–13101.
- (40) Guihaumé, J.; Halbert, S.; Eisenstein, O.; Perutz, R. N. Hydrofluoroarylation of Alkynes with Ni Catalysts. C–H Activation Via Ligand-to-Ligand Hydrogen Transfer, an Alternative to Oxidative Addition. *Organometallics* **2012**, *31*, 1300–1314.
- (41) Elsby, M. R.; Johnson, S. A. Nickel-Catalyzed C–H Silylation of Arenes with Vinylsilanes: Rapid and Reversible B–Si Elimination. *J. Am. Chem. Soc.* **2017**, *139*, 9401–9407.
- (42) Saper, N. I.; Ohgi, A.; Small, D. W.; Semba, K.; Nakao, Y.; Hartwig, J. F. Nickel-Catalyzed Anti-Markovnikov Hydroarylation of Unactivated Alkenes with Unactivated Arenes Facilitated by Non-Covalent Interactions. *Nat. Chem.* **2020**, *12*, 276–283.
- (43) Hartwig, J. F. *Organotransition Metal Chemistry: From Bonding to Catalysis*; University Science Books: Mill Valley, CA, 2010.
- (44) Sakata, K.; Eda, M.; Kitaoka, Y.; Yoshino, T.; Matsunaga, S. Cp*CoIII-Catalyzed C–H Alkenylation/Annulation Reactions of Indoles with Alkynes: A Dft Study. *J. Org. Chem.* **2017**, *82*, 7379–7387.
- (45) Ikemoto, H.; Yoshino, T.; Sakata, K.; Matsunaga, S.; Kanai, M. Pyrroloindolone Synthesis Via a Cp*CoIII-Catalyzed Redox-Neutral Directed C–H Alkenylation/Annulation Sequence. *J. Am. Chem. Soc.* **2014**, *136*, 5424–5431.
- (46) Hummel, J. R.; Ellman, J. A. Cobalt(III)-Catalyzed Synthesis of Indazoles and Furans by C–H Bond Functionalization/Addition/Cyclization Cascades. *J. Am. Chem. Soc.* **2015**, *137*, 490–498.
- (47) Gao, K.; Lee, P.-S.; Fujita, T.; Yoshikai, N. Cobalt-Catalyzed Hydroarylation of Alkynes through Chelation-Assisted C–H Bond Activation. *J. Am. Chem. Soc.* **2010**, *132*, 12249–12251.
- (48) Gao, K.; Yoshikai, N. Regioselectivity-Switchable Hydroarylation of Styrenes. *J. Am. Chem. Soc.* **2011**, *133*, 400–402.
- (49) Lee, P. S.; Yoshikai, N. Aldimine-Directed Branched-Selective Hydroarylation of Styrenes. *Angew. Chem. Int. Ed.* **2013**, *52*, 1240–1244.
- (50) Xu, W.; Yoshikai, N. N–H Imine as a Powerful Directing Group for Cobalt-Catalyzed Olefin Hydroarylation. *Angew. Chem. Int. Ed.* **2016**, *55*, 12731–12735.
- (51) Ding, Z.; Yoshikai, N. Mild and Efficient C2-Alkenylation of Indoles with Alkynes Catalyzed by a Cobalt Complex. *Angew. Chem. Int. Ed.* **2012**, *51*, 4698–4701.
- (52) Xu, W.; Pek, J. H.; Yoshikai, N. Cobalt-Catalyzed, Imine-Directed Olefin Hydroarylation under Grignard-Free Conditions. *Adv. Synth. Catal.* **2016**, *358*, 2564–2568.
- (53) Gao, K.; Yoshikai, N. Cobalt–Phenanthroline Catalysts for the Ortho Alkylation of Aromatic Imines under Mild Reaction Conditions. *Angew. Chem. Int. Ed.* **2011**, *50*, 6888–6892.
- (54) Gandeepan, P.; Muller, T.; Zell, D.; Cera, G.; Warratz, S.; Ackermann, L. 3d Transition Metals for C–H Activation. *Chem Rev* **2019**, *119*, 2192–2452.
- (55) Sanjosé-Orduna, J.; Gallego, D.; Garcia-Roca, A.; Martin, E.; Benet-Buchholz, J.; Pérez-Temprano, M. H. Capturing Elusive Cobaltcycle Intermediates: A Real-Time Snapshot of the Cp*CoIII-Catalyzed Oxidative Alkyne Annulation. *Angew. Chem. Int. Ed.* **2017**, *56*, 12137–12141.
- (56) Sanjosé-Orduna, J.; Benet-Buchholz, J.; Pérez-Temprano, M. H. Unravelling Molecular Aspects of the Migratory Insertion Step in Cp*CoIII Metallacyclic Systems. *Inorg. Chem.* **2019**, *58*, 10569–10577.
- (57) Fallon, B. J.; Derat, E.; Amatore, M.; Aubert, C.; Chemla, F.; Ferreira, F.; Perez-Luna, A.; Petit, M. C–H Activation/Functionalization Catalyzed by Simple, Well-Defined Low-Valent Cobalt Complexes. *J. Am. Chem. Soc.* **2015**, *137*, 2448–2451.
- (58) Wakatsuki, Y.; Yamazaki, H.; Lindner, E.; Bosamle, A. (1, 3-Butadiene-1, 4-Diyl)(H5-Cyclopentadienyl)-(Triphenylphosphine)Cobalt with Various Substituents in *Inorganic Syntheses*; Kaesz, H. D., Ed.; Wiley: New York, 1989; Vol. 26, pp 189–200.
- (59) Sacco, A.; Rossi, M. Hydride and Nitrogen Complexes of Cobalt. *Chem. Commun.* **1967**, 316–316.
- (60) Yamamoto, A.; Kitazume, S.; Pu, L. S.; Ikeda, S. Synthesis and Properties of Hydridodinitrogentris(Triphenylphosphine)Cobalt(II) and the Related Phosphine-Cobalt Complexes. *J. Am. Chem. Soc.* **1971**, *93*, 371–380.
- (61) Halbritter, G.; Knoch, F.; Wolski, A.; Kisch, H. Functionalization of Aromatic Azo Compounds by the Cobalt-Catalyzed, Regioselective Double Addition of Tolane: 2,6-Distilbenzylazobenzenes and 2,3-Dihydrocinnolines. *Angew. Chem. Int. Ed.* **1994**, *33*, 1603–1605.
- (62) Morris, R. H. Estimating the Acidity of Transition Metal Hydride and Dihydrogen Complexes by Adding Ligand Acidity Constants. *J. Am. Chem. Soc.* **2014**, *136*, 1948–1959.
- (63) Morris, R. H. Brønsted–Lowry Acid Strength of Metal Hydride and Dihydrogen Complexes. *Chem. Rev.* **2016**, *116*, 8588–8654.
- (64) Kosar, W. Grignard Reagents as Bases in *Handbook of Grignard Reagents*; Silverman, G. S., Rakita, P. E., Eds.; Marcel Dekker, Inc.: New York, 1996; pp 441–454.
- (65) Yamamoto, A.; Miura, Y.; Ito, T.; Chen, H. L.; Iri, K.; Ozawa, F.; Miki, K.; Sei, T.; Tanaka, N.; Kasai, N. Preparation, X-Ray Molecular Structure Determination, and Chemical Properties of Dinitrogen-Coordinated Cobalt Complexes Containing Triphenylphosphine Ligands and Alkali Metal or Magnesium. Protonation of the Coordinated Dinitrogen to Ammonia and Hydrazine. *Organometallics* **1983**, *2*, 1429–1436.
- (66) Reich, H. J.; Kulicke, K. J. Dynamics of Solvent Exchange in Organolithium Reagents. Lithium as a Center of Chirality. *J. Am. Chem. Soc.* **1996**, *118*, 273–274.
- (67) Reich, H. J. What’s Going on with These Lithium Reagents? *J. Org. Chem.* **2012**, *77*, 5471–5491.
- (68) Reich, H. J.; Sikorski, W. H.; Sanders, A. W.; Jones, A. C.; Plessel, K. N. Multinuclear NMR Study of the Solution Structure and Reactivity of Tris(trimethylsilyl)methylolithium and Its Iodine Ate Complex. *J. Org. Chem.* **2009**, *74*, 719–729.
- (69) Apps, S. L.; Miller, P. W.; Long, N. J. Cobalt(-I) Triphos Dinitrogen Complexes: Activation and Silyl-Functionalisation of N₂. *Chem. Commun.* **2019**, *55*, 6579–6582.
- (70) Gao, Y.; Li, G.; Deng, L. Bis(Dinitrogen)Cobalt(-I) Complexes with Nhc Ligation: Synthesis, Characterization, and Their Dinitrogen Functionalization Reactions Affording Side-on Bound Diazene Complexes. *J. Am. Chem. Soc.* **2018**, *140*, 2239–2250.
- (71) Kreyenschmidt, F.; Meurer, S. E.; Koszinowski, K. Mechanisms of Cobalt/Phosphine-Catalyzed Cross-Coupling Reactions. *Chem. Eur. J.* **2019**, *25*, 5912–5921.
- (72) Barton, J. S. A Comprehensive Enzyme Kinetic Exercise for Biochemistry. *J. Chem. Educ.* **2011**, *88*, 1336–1339.
- (73) Pratt, C. W.; Cornely, K. Enzyme Kinetics and Inhibition in *Essential Biochemistry*; 3rd ed.; Wiley: Hoboken, NJ, 2014; p 188–220.
- (74) Marin, G. B.; Yablonsky, G. S.; Constales, D. *Kinetics of Chemical Reactions*; Wiley-VCH: Weinheim, Germany, 2011.

- (75) Lail, M.; Bell, C. M.; Conner, D.; Cundari, T. R.; Gunnoe, T. B.; Petersen, J. L. Experimental and Computational Studies of Ruthenium(II)-Catalyzed Addition of Arene C–H Bonds to Olefins. *Organometallics* **2004**, *23*, 5007-5020.
- (76) Albright, T. A.; Gordon, M. D.; Freeman, W. J.; Schweizer, E. E. Nuclear Magnetic Resonance Studies. 5. Properties of Phosphorus-Carbon Ylides. *J. Am. Chem. Soc.* **1976**, *98*, 6249-6252.
- (77) Chin, C. S.; Park, Y.; Kim, J.; Lee, B. Facile Insertion of Alkynes into Ir–P (Phosphine) and Ir–As (Arsine) Bonds: Second and Third Alkyne Addition to Mononuclear Iridium Complexes. *J. Chem. Soc., Chem. Commun.* **1995**, 1495-1496.
- (78) Huggins, J. M.; Bergman, R. G. Mechanism, Regiochemistry, and Stereochemistry of the Insertion Reaction of Alkynes with Methyl(2,4-Pentanedionato)(Triphenylphosphine)Nickel. A Cis Insertion That Leads to Trans Kinetic Products. *J. Am. Chem. Soc.* **1981**, *103*, 3002-3011.
- (79) Yang, K.; Bott, S. G.; Richmond, M. G. Intramolecular Phosphine Attack on a Coordinated Alkyne Ligand in $\text{Co}_2(\text{CO})_4(\text{bma})(\mu\text{-PhCCH})$. Characterization of the Zwitterionic Hydrocarbyl Complex $\text{Co}_2(\text{CO})_4[\mu\text{-}\eta^2\text{:}\eta^2\text{:}\eta^1\text{-PhC=C(H)PPh}_2\text{C=C(PPh}_2\text{)C(O)OC(O)}]$. *Organometallics* **1994**, *13*, 3767-3769.
- (80) A. Fairhurst, S.; L. Hughes, D.; Marjani, K.; L. Richards, R. Insertion of Alkynes into Molybdenum–Phosphine and –Carbon Bonds. Crystal Structures of the Alkyne–Ylide Complex $[\text{MoO}(\text{SC}_6\text{H}_2\text{Pr}^i\text{-2,4,6})_2\{\eta^2\text{-CHC(Tol)}\}\{\text{C(Tol)CHPMePh}_2\}]$ (Tol = $\text{C}_6\text{H}_4\text{Me-4}$) and the Phosphonium–Alkylidene Complex $[\text{MoO}(\text{SC}_6\text{H}_2\text{Pr}^i\text{-2,4,6})_3\{\text{C(Ph)CH=C(Ph)CH}_2\text{PMe}_2\text{Ph}\}]$. *J. Chem. Soc., Dalton Trans.* **1998**, 1899-1904.
- (81) Hoffman, D. M.; Huffman, J. C.; Lappas, D.; Wierda, D. A. Alkyne Reactions with Rhenium(V) Oxo Alkyl Phosphine Complexes - Phosphine Displacement Versus Apparent Re-P Insertion. *Organometallics* **1993**, *12*, 4312-4320.
- (82) Allen, A.; Lin, W. Unprecedented Insertion of Alkynes into a Palladium–Phosphine Bond. A Facile Route to Palladium-Bound Alkenyl Phosphorus Ylides. *Organometallics* **1999**, *18*, 2922-2925.
- (83) Takats, J.; Washington, J.; Santarsiero, B. D. Condensation of $\text{Os}(\text{CO})_4(\eta^2\text{-HCCH})$ with $\text{CpRh}(\text{CO})(\text{PR}_3)$. Unexpected Phosphine Dependence in the Formation of Dimetallacycles: Reverse Regiochemistry and a Zwitterionic Compound. *Organometallics* **1994**, *13*, 1078-1080.
- (84) Simmons, E. M.; Hartwig, J. F. On the Interpretation of Deuterium Kinetic Isotope Effects in C–H Bond Functionalizations by Transition-Metal Complexes. *Angew. Chem. Int. Ed.* **2012**, *51*, 3066-3072.
- (85) Wang, L.; Carrow, B. P. Oligothiophene Synthesis by a General C–H Activation Mechanism: Electrophilic Concerted Metalation–Deprotonation (Ecmd). *ACS Catal.* **2019**, *9*, 6821-6836.
- (86) Lam, W. H.; Jia, G.; Lin, Z.; Lau, C. P.; Eisenstein, O. Theoretical Studies on the Metathesis Processes, $[\text{Tp}(\text{PH}_3)\text{MR}(\eta^2\text{-H-CH}_3)] \rightarrow [\text{Tp}(\text{PH}_3)\text{M}(\text{CH}_3)(\eta^2\text{-H-R})]$ (M=Fe, Ru, and Os; R=H and CH_3). *Chem. Eur. J.* **2003**, *9*, 2775-2782.
- (87) Lapointe, D.; Fagnou, K. Overview of the Mechanistic Work on the Concerted Metallation–Deprotonation Pathway. *Chem. Lett.* **2010**, *39*, 1118-1126.
- (88) Yamazaki, K.; Obata, A.; Sasagawa, A.; Ano, Y.; Chatani, N. Computational Mechanistic Study on the Nickel-Catalyzed C–H/N–H Oxidative Annulation of Aromatic Amides with Alkynes: The Role of the Nickel (0) Ate Complex. *Organometallics* **2018**, *38*, 248-255.
- (89) Ma, P.; Chen, H. Ligand-Dependent Multi-State Reactivity in Cobalt(III)-Catalyzed C–H Activations. *ACS Catal.* **2019**, *9*, 1962-1972.
- (90) Schipper, D. J.; Hutchinson, M.; Fagnou, K. Rhodium(III)-Catalyzed Intermolecular Hydroarylation of Alkynes. *J. Am. Chem. Soc.* **2010**, *132*, 6910-6911.
- (91) Herbert, M. B.; Suslick, B. A.; Liu, P.; Zou, L.; Dornan, P. K.; Houk, K. N.; Grubbs, R. H. Cyclometalated Z-Selective Ruthenium Metathesis Catalysts with Modified N-Chelating Groups. *Organometallics* **2015**, *34*, 2858-2869.
- (92) Schmidt, A.; Nödling, A. R.; Hilt, G. An Alternative Mechanism for the Cobalt-Catalyzed Isomerization of Terminal Alkenes to (Z)-2-Alkenes. *Angew. Chem. Int. Ed.* **2015**, *54*, 801-804.
- (93) Werner, H.; Wolf, J.; Schubert, U.; Ackermann, K. Basische Metalle: Lviii. Vinylrhodium-Komplexe Durch Protonierung Der Alkin-Verbindungen $\text{C}_5\text{H}_5\text{Rh}(\text{C}_2\text{Ph}_2)\text{PPr}_3^i$ Und $\text{C}_5\text{H}_5\text{Rh}(\text{PhC}_2\text{H})\text{PPr}_3^i$. Molekül-Und Kristallstruktur Von $\text{C}_5\text{H}_5\text{Rh}(\text{E-CPh=CHPh})(\text{PPr}_3)\text{OCOCF}_3$ Und Des Metallacyclus $\text{C}_5\text{H}_5(\text{PPr}_3)\text{RhC}_6\text{H}_4\text{CH=CPh}$. *J. Organomet. Chem.* **1986**, *317*, 327-356.



1
2
3
4
5
6
7
8
9
10
11
12
13
14
15
16
17
18
19
20
21
22
23
24
25
26
27
28
29
30
31
32
33
34
35
36
37
38
39
40
41
42
43
44
45
46
47
48
49
50
51
52
53
54
55
56
57
58
59
60